UMCES

University of Maryland Center for Environmental Science

Chesapeake Biological Laboratory

Comprehensive Assessment of the Impacts of Large Reductions in Point Source Nutrient Loading to the Patapsco and Back River Estuaries

Final Report

Prepared for: Maryland Department of the Environment

October 2022

Ref. No. [UMCES]CBL 2022-010

Comprehensive Assessment of the Impacts of Large Reductions in Point Source Nutrient Loading to the Patapsco and Back River Estuaries

Participants:

J. M. Testa[1] Co-Principal Investigator
W. R. Boynton[1] Co-Principal Investigator
C. L. S. Hodgkins[1] Senior Faculty Research Assistant

FINAL REPORT
Prepared for:

MDE

October 2022

[1] University of Maryland Center for Environmental Science

Chesapeake Biological Laboratory (CBL)

PO Box 38, 146 Williams Street

Solomons, MD 20688-0038

Technical Report Series No. TS-785-22 of the University of Maryland Center for Environmental Science.

Contents

Introduction

Background

Eutrophication, or the enhanced input of organic matter to aquatic ecosystems, remains a pressing social problem that is associated with declines in oxygen availability, the loss of submerged macrophyte habitats, and the proliferation of harmful phytoplankton blooms. Recognition of this problem has led to expensive and expansive socio-economic commitments to reduce the inputs of bioavailable nutrients that commonly support elevated phytoplankton biomass and associated bottom water and sediment degradation. Although initial efforts to mitigate eutrophication were difficult to associate with clear improvements in tidal waters (e.g., Duarte et al. 2009), sustained nutrient reductions and investments in improved wastewater treatment technologies have led to substantial declines in eutrophication in a growing number of estuaries (e.g., Boynton et al. 2014, Taylor et al. 2011, Stæhr et al. 2017, Testa et al. 2022).

Substantial investments made to upgrade Maryland wastewater treatment plants (WWTPs) during the past several decades have significantly reduced the amount of nitrogen and phosphorus being discharged into Chesapeake Bay tidal waters. Several case studies (Boynton et al. 2014, Fisher et al. 2021, Testa et al. 2022) have documented how these upgrades have ultimately led to the expected improvements in some aspects of water quality (e.g., reduced chlorophyll-a, turbidity). Statistical modeling of mainstem Chesapeake Bay hypoxia has also recently incorporated wastewater nutrient inputs to tidal waters, where model predictions of hypoxic volume improved when wastewater loads were included (Scavia et al. 2021). Given that wastewater nutrient load reductions in Bay tributaries have led to reduced nutrient flux to the mainstem Chesapeake Bay (Testa et al. 2022), tributary sewage treatment upgrades should have an impact on mainstem water quality. However, the magnitude of these improvements, the time it takes for water quality responses to emerge, and the assortment of metrics used to evaluate system response have been different across tributaries and within the mainstem Bay. These differences emerge because of (1) limited data availability, (2) differences in the physical nature of the tributary or the extent of its eutrophication history, and (3) discrepancies in the relative contribution of WWTP nutrient loads to overall nutrient loads.

Thus, the purpose of this report is to quantify both the ecosystem response of the Patapsco River estuary to long-term WWTP load reductions and also the effects of recent WWTP load reductions on the Back River estuary water quality. We also evaluated the potential for failed sewage treatment operations during part of 2021 and 2022 in the Patapsco and Back River WWTPs to impact water quality, including the reversal of water quality improvements in the Back River. These estuaries are ideal locations for this type of analysis, given the substantial magnitude of WWTP nutrient load reduction, the dominance of WWTP loads in the overall nutrient input budget, and a wealth of available data that can be used to examine (1) nutrient, chlorophyll-a, and oxygen concentration changes during multiple decades, (2) rates of nutrient recycling in sediments and the water-column, (3) physical transport and nutrient input-output budgets for the estuary, and (4) rates of organic matter production (i.e., ecosystem metabolism).

Data Sources and Methods

In this report, we combined analysis of historical data, numerical modeling, and diagnostic mass balance computations to comprehensively assess estuarine water quality changes in response to WWTP load reductions. Specifically, we collated model estimates of nutrient input from the watershed, wastewater treatment plant (WWTP) nutrient loads, and water-column nutrient and chlorophyll-a data collected by the Maryland Department of the Environment, the Department of Natural Resources, and the Chesapeake Bay Program. This evaluation provides information necessary to diagnose the current and future water quality conditions of an estuary, an exercise that typically involves developing, testing and using, in a forecasting mode, various water quality models.

Non-point and Point Source Nutrient Loads and Flow

We assembled freshwater and nutrient loading rates from the Patapsco River WWTP and other relevant point source inputs, as well as loads estimated for the PATMH segment of the Phase 6 Chesapeake Bay Program watershed model to compute the magnitude and temporal pattern of change in loadings to the estuary since 1985. We used these data to make estimates of both point and non-point watershed freshwater, nitrogen (NH_4, NO_{23} and Total Nitrogen (TN)) and phosphorus (PO_4 and Total Phosphorus (TP)) inputs to the Patapsco River estuary during the 1985-2020 time period. Annual WWTP inputs directly to the Patapsco River from the Patapsco River and Cox Creek WWTPs (as well as the former Sparrows Point plant and W.R. Grace facility) were sourced from The National Pollutant Discharge Elimination System (NPDES) data and nutrient concentration time-series collated by the Maryland Department of the Environment and Chesapeake Bay Program.

Tidal Water Quality

We analyzed tidal water-quality monitoring data from long-term Maryland Department of Natural Resources stations WT5.1, CB3.2, and WT4.1 (1985-2021; Figure 1) to assess temporal trends in water-quality. These data are collected at bi-weekly or monthly intervals at multiple depths. We focused on concentrations of nitrogen (NH_4, NO_{23} and Total Nitrogen (TN)), phosphorus (PO_4 and Total Phosphorus (TP)), dissolved oxygen, salinity, and chlorophyll-a. We also analyzed the 1985-2020 time-series of dissolved oxygen concentration and water temperature profiles measured at WT5.1 to examine changes in low oxygen conditions (hypoxia). For oxygen data, we interpolated monthly concentrations at each depth to daily estimates, and calculated the total number of days that oxygen was below several threshold values relevant to water quality criteria (0.5, 3.2, and 5 mg/L). For water temperature, we interpolated monthly concentrations at each depth to daily estimates, and calculated the total number of days that temperature was above several threshold values (20, 22, 24, 26, and 28 ^{o}C).

Ecosystem Metabolism

We estimated ecosystem gross primary production, respiration, and net ecosystem metabolism (NEM) from observed continuous (15-minute) time-series of O_2 at all past and current continuous monitoring stations within the Patapsco River (Figure 1, Table 1). The original concept and method for computing gross GPP and respiration (and NEM) was developed in the 1950s (Odum and Hoskin 1958) and has subsequently been modified for a variety of aquatic ecosystems (Caffrey 2004). The approach derives ecosystem rates of gross primary production (P_g = GPP) and respiration (R_t) from increases in O_2 concentrations during daylight hours and declines during nighttime hours, respectively. The sum of these two processes over 24 h, after correcting for air-sea exchange, provides an estimate of NEM. We used continuous O_2 concentration measurements at continuous monitoring stations in the Patapsco River estuary from times covering 2004 through 2021 (Figure 1) to apply a modified approach (Beck et al. 2015), which uses a weighted regression to remove tidal effects on O_2 time-series since the tide can advect higher or lower O_2 past the sensor thereby influencing the calculation of NEM. The changes in O_2 used to compute metabolic rates were corrected for air-water gas exchange using the equation $D = K_a (C_s\text{-}C)$, where D is the rate of air-water O_2 exchange (mg O_2 L^{-1} h^{-1}), K_a is the volumetric aeration coefficient (h^{-1}), and C_s and C are the O_2 saturation concentration and observed O_2 concentration (mg O_2 L^{-1}), respectively. K_a was computed as a function of wind speed derived from the North American Land Data Assimilation System (NLDAS) and details of the air-water gas calculation are incorporated into the R package WtRegDO (Beck et al. 2015) and described in detail elsewhere (Thébaultet al. 2008). The calculations utilized salinity, temperature, and O_2 times-series from the sensors at each platform. Tidal height, atmospheric pressure, and air temperature data were obtained from a nearby NOAA station at Baltimore, Maryland (https://tidesandcurrents.noaa.gov/stationhome.html?id=8574680). Any gaps in data were filled in the tides and meteorological data from Tolchester Beach, Maryland (https://tidesandcurrents.noaa.gov/stationhome.html?id=8573364). The O_2 data used to make metabolic computations were obtained from sensors deployed near-bottom in relatively shallow waters (Table 1) that were well-mixed, which is necessary for the air-water flux correction to be valid and for the O_2 time-series to be representative of the combined water-column and sediments (Murrell et al. 2018).

Sediment Flux Model

We synthesized previously measured rates of sediment-water exchanges (Boynton et al., unpublished) of dissolved nutrients and oxygen combined with the implementation of a sediment flux model (SFM) during a three decade period (1985-2020) to estimate sediment impacts on water quality and denitrification rates. Measured rates of Patapsco River sediment-water fluxes of nutrients (NH_4, NO_{23}, PO_4) and oxygen have been made at several times and locations over the last several decades (Figure 1). We used these measurements to constrain a 2-layer sediment biogeochemical model (SFM) that has been widely applied and validated in Chesapeake Bay (Brady et al. 2013, Testa et al. 2013) to examine the biogeochemical response of the sediments altered organic matter availability. The model structure for SFM involves 4 general processes: (1) the sediment receives depositional fluxes of POM (particulate organic matter), as well as biogenic and inorganic phosphorus and silica from the overlying water, (2) the decomposition of POM produces soluble intermediates that are quantified as diagenesis fluxes, (3) solutes react, transfer between solid and dissolved phases, are transported between the aerobic and anaerobic layers of the sediment, or are released as gases (CH_4, N_2), and (4) solutes are returned to the overlying water as sediment-water fluxes (NH_4, NO_{23}, PO_4, O_2). SFM numerically integrates mass-balance equations for chemical constituents in 2 functional layers: an aerobic layer near the sediment–water interface of variable depth (H1) and an anaerobic layer below that is equal to the total modeled sediment depth (0.1 m) minus the depth of H1. The model includes an algorithm that continually updates the thickness of the aerobic layer (H1) at a simulation time-step of 1 h, where output is aggregated at 1 day intervals. The diagenesis of POM is modeled by partitioning the settling POM into 3 reactivity classes, termed the G model, where each class represents a fixed portion of the organic material that reacts at a specific rate. Further details on the model and it implementation can be found elsewhere (Testa et al. 2013). To develop a time-series of organic carbon, nitrogen, and phosphorus (POM) deposition associated with reductions in phytoplankton biomass and reduced organic matter input from the Patapsco River WWTP, we developed a series of simulations during the 1985-2020 period. We estimated POM deposition from the overlying water chlorophyll-a concentration by converting chlorophyll-a to carbon (assuming C:CHL = 60) and assuming a sinking rate of algal biomass of 0.5 m d^{-1}. We ran simulations calibrated to data at stations in the middle region of the Patapsco estuary near WT5.1 and in the inner harbor.

Nutrient Budget

We synthesized the loading, concentration, and model simulation data collated and generated during this analysis to generate whole-system nitrogen (N) and phosphorus (P) budgets for the Patapsco estuary (Figure 18). We will use this approach to identify (1) how much of the WWTP input is retained in the Patapsco estuary/exported to Chesapeake Bay, (2) have WWTP reductions significantly changed the overall nutrient inputs to the system, (3) is sediment recycling a large potential delay on water quality improvements, and (4) how much of the internal load is lost to denitrification. We chose three time periods to develop these budgets, including a period during intense point-source nutrient loading (1985-1990), a period following large reductions in industrial nutrient loading (2010-2014), and a period following the implantation of ENR at the Patapsco River WWTP (2019-2020). The diffuse and point source N and P loads were obtained from the Phase six dynamic watershed model loads to the mesohaline Patapsco water quality segment, which represents the tidal estuary. Atmospheric nitrogen deposition was estimated from the Wye River station in the National Atmospheric Deposition Program (NADP). Total nitrogen and phosphorus concentrations in the water-column were computed by multiplying the depth-averaged concentrations at WT5.1 by the volume of the estuary. While this single station does not represent every region of the estuary, comparisons of the WT5.1 station with data measured by MDE between 2016 to 2019 (nutrients, chlorophyll-a; data provided in supplemental materials) suggest that this is a reasonable representation of the system. We also estimated four properties of the sediment from a combination of observed sediment-water fluxes and modeled estimates of sediment-water NH_4 and PO_4 fluxes, nutrient burial, denitrification, and sediment N and P content. We provide two estimates of these values in Figure 18, separated by a forward slash, where the first estimate was an observation-based estimate based upon prior analysis or a limited amount of data (Boynton et al., unpublished) and the second value is estimated from the long-term SFM simulation described above. Finally, we used estimates of net exchange of N and P across the mouth of the Patapsco from the Chesapeake Bay Program Water Quality and Sediment Transport Model (WQSTM) from the years 1985-2010 to estimate the net exchange of N and P across the seaward boundary. We made a separate estimate of these exchange terms with the box model described above. All units are in kilograms per year.

Salt and Water Balance Budget

We constructed a simple salt-and water-balance 'box model' to estimate water and nutrient exchange and export from the Patapsco River estuary to/with Chesapeake Bay and changes in the ecosystem-scale net retention of nitrogen and phosphorus by the Patapsco estuary. This approach involves estimating the net exchange of nitrogen and phosphorus from the Patapsco River to the upper Chesapeake Bay during the 1985-2020 period. Quantification of this exchange allows for an assessment of (1) whether the upper Chesapeake Bay is an additional source of nutrients to drive long-term change in the Patapsco River, or (2) if WWTP reductions in the Patapsco River led to a substantial reduction in overall nutrient export to Chesapeake Bay. The latter feature is important for understanding how nutrient processing within tributary estuaries may modulate the effect of nutrient reductions on the biogeochemistry of Chesapeake Bay overall. To do this, we will compute the Patapsco River's time-dependent, seasonal mean circulation using salinity and freshwater input data. This box modeling approach computes advective and diffusive exchanges of water and salt between adjacent control volumes (which are assumed to be well mixed) and across end-member boundaries using the solution to non-steady state equations balancing salt and water inputs, outputs, and storage changes (Officer 1980, Hagy et al. 2000). Despite prior research that reveals that the Patapsco estuary has both 2-layer and 3-layer circulation, we decided to treat the Patapsco River as a single volume and characterize the salinity (and nutrients) within the estuary from the long-term monitoring station at WT5.1 (Figure 1). Total watershed inputs of freshwater and nutrients were obtained from the Phase 6 model inputs. The seaward boundary concentrations will be derived from a long-term monitoring station in the upper Chesapeake Bay (CB3.2; Figure 1). Estuarine area and volume were obtained from Cronin and Pritchard (1975). Details of the salt and water balance computation and nutrient export are included in many prior publications where we have successfully applied this approach to answer questions regarding water quality responses to WWTP upgrades (Testa et al. 2008, Stæhr et al. 2017, Testa et al. 2022).

Results

Here we present the primary results of our study of the Patapsco River estuary response to wastewater treatment plant load reductions. We analyzed far more data than presented here, and we include the raw data and select illustrations of those data as a supplemental package included with this report.

Non-Point and Point Source Nutrient Loads and Flow

Annual nitrogen (dissolved inorganic nitrogen (DIN) and total nitrogen (TN)) and phosphorous (dissolved inorganic phosphorous (DIP) and total phosphorous (TP)) loads and flow to the Patapsco River are from 1985 to 2020 are shown in Figure 3. TN loads declined from ~ 7 million to just over 2 million kg year^{-1} with a pulse of ~ 5 million kg year^{-1} in 2015. TP and DIP loads declined from ~400,000 to ~180,000 kg year^{-1} and ~220,000 to ~50,000 kg year^{-1}, respectively. TP and DIP also showed an increase in load in 2015 which then returned to lower values in subsequent years.

Annual point source nitrogen (NH_4, NO_{23}, and Total Nitrogen (TN)) and phosphorus (PO_4 and Total Phosphorus (TP)) loads from the Cox Creek (1985-2020) and Patapsco (1985-2016) Waste

Water Treatment Plant (WWTP) are shown in Figure 4. PO_4 and TP loads at Cox Creek declined steadily from 1991 to 2016 and then rapidly decreased from 2016 to 2018. Cox Creek nitrogen loads were more variable with NO_{23} varying moderately over the entire time series, while NH_4 and TN were variable earlier in the time series and then declined after 2003.TN and NH_4 loads at the Patapsco WWTP increased from roughly 2000 to 4000 kg day^{-1} and NO_{23} loads remained less than 500 kg day^{-1} for the length of the record. Patapsco WWTP TP and PO_4 loads decreased from 500 (TP) and 350 (PO_4) kg day^{-1} in 1985 to ~220 (TP) and ~ 50 (PO_4) kg day^{-1} in 1989 and were variable at ~200 kg TP day^{-1} and ~100 kg day^{-1} of PO_4 from 1989 to 2017.

Interestingly, Phase 6 model estimates of total point source nitrogen and phosphorus loads over the 1985 to 2020 period indicate extensive and consistent long-term declines (Figure 5). These large declines are not consistent in magnitude with the Cox Creek declines and are not consistent in pattern with the Patapsco WWTP time-series. In fact, the Patapsco WWTP TN and TP load is a small fraction of total point source loads in the Patapsco segment until the mid-2000s, after which the Patapsco WWTP becomes the dominant point source (Figure 5). Using NPDES municipal and industrial discharge information, it was clear that the large decline in TN and TP load since 1985 was primarily driven by reductions in loads from two industrial facilities, including Sparrows Point in the late 1980s and the W.R. Grace facility from the 1980s and 1990s (Figure 6; Gopal Bhatt personal communication).

Tidal Water Quality comparisons at Patapsco station WT5.1 and Chesapeake Bay station CB3.2

Various forms of nitrogen and phosphorus in surface waters at the long-term sentinel station (WT5.1) are shown for the period 1985 – 2022 in Figures 7&8. Over the course of this record surface TN concentrations declined from almost 120 µM to about 70 µM during summer of 2020. Although long-term declines from 1985-2022 were only evident in surface waters during summer for NO_{23}, NH_4 declines were substantial in both surface and bottom waters and both annually and during summer. Following the wastewater treatment plant failures beginning in late 2020, TN and NO_2+NO_3 concentrations were somewhat elevated. These temporal patterns of nitrogen concentration declines are well correlated with nitrogen load reductions (Figure 9). For comparison, there were not comparable declines in nitrogen concentrations in the adjacent Chesapeake Bay station for any nitrogen species (Figure 7).

Concentration declines in phosphorus were also evident at the sentinel site and consistent with (and correlated to) long-term phosphorus load declines (Figure 8&9). Surface water phosphorus concentrations at WT5.1 (especially PO_4) were lowest at the end of the data record, and were comparable or lower than concentrations in the adjacent mainstem Bay by 2020. In fact, mainstem Bay P concentrations increased over the 1985-2022 period while Patapsco concentrations declined. Bottom water phosphorus concentration declines were more modest than surface water, and were more variable from year to year (Figure 8).

To place the relationships between nitrogen load and Patapsco and Back River nitrogen concentration within the context of other Chesapeake Bay environments, we plotted period-specific TN concentrations against TN loads for the mainstem Chesapeake Bay, Patuxent estuary, Potomac estuary, Choptank estuary, and the Patapsco and Back River estuaries (Figure

10). These comparisons reveal a consistent linear relationship between nitrogen load and concentration across the systems, but a larger slope for the Back River across wastewater treatment regimes and a smaller slope across time in the Patapsco estuary (i.e., smaller concentration reduction for a given load reduction). This persistence of higher nitrogen concentrations is related to the fact that sediment-water N fluxes for a given nitrogen load are high relative to other Chesapeake Bay systems, and much higher than the adjacent Back River estuary (Figure 10).

Chlorophyll-a concentrations recorded at the sentinel station (WT5.1) are shown for the period of record in Figure 11. Summer and annual-mean chlorophyll-a concentrations were highly variable in the Patapsco estuary over time, ranging from about 25 (2018-2022) to over 100 $\mu g\ l^{-1}$ (1987) and in most years ranged between 25 and 75 $\mu g\ l^{-1}$. Clearly, other factors, in addition to nutrient loads and concentrations, played into generating chlorophyll-a concentration patterns. However, chlorophyll-a concentrations during summer declined over the entire record, with the lowest concentrations in 2019 and 2020. In 2021, a large bloom reappeared in both surface and bottom waters. At the adjacent mainstem site, chlorophyll-a concentrations increased since 1985 and became comparable in magnitude to Patapsco River concentrations by 2018-2022 (Figure 11). Interestingly, bottom-layer chlorophyll was highly variable in both the mainstem and the Patapsco River estuary, and the chlorophyll-a concentrations at the two locations were highly correlated ($r^2 = 0.73$; Figure 12).

Metrics of dissolved oxygen concentration showed potential long-term changes that require additional analyses. The number of days that oxygen was below 0.5 mg/L was variable from 1985-2020, but there was a slight deepening of the region where this very low oxygen occurred, except for a period during the extremely high flow period of 2018-2019 (Figure 13). In general this low oxygen water was restricted to below 10 meters. In contrast, it appeared that the number of days oxygen was below 5 mg/L increased in the mid-depths (5-10 m) over the period of record (Figure 13), as it also did for oxygen less than 2 mg/L (data not shown). This increase in the duration of oxygen below 5 mg/L, the 30-day dissolved oxygen criteria for Chesapeake Bay water quality, corresponded to an increase in the number of days where temperature was above 24 degrees C Figure 14).

Patapsco River Ecosystem Metabolism

Estimates of ecosystem gross primary production (Pg), respiration (Rt), and net ecosystem metabolism (NEM) derived from six locations in the Patapsco River were highly variable over time and included high rates (Figure 15). The magnitude of the rates followed a spatial pattern in the estuary, where rates were highest in the inner harbor (Pg and Rt averaged ~1000 mmol $O_2\ m^{-2}\ d^{-1}$ and peaked at > 2000), moderate at Masonville Cove and Fort McHenry (Pg and Rt averaged ~500 mmol $O_2\ m^{-2}\ d^{-1}$ and did not exceed 1000), and was lowest at Fort Armisted and Fort Smallwood (Pg and Rt < 500 mmol $O_2\ m^{-2}\ d^{-1}$). At Masonville Cove, which had the longest time-series, interannual variability in metabolic rates did not indicate any long-term changes since 2009, but indicated a strong relationship with freshwater flow into the Patapsco estuary. In this case, years with higher river flow were associated with lower metabolic rates (Figure 16), including a negative relationship of Pg and Rt to flow ($r^2 = 0.59$ ad 0.55, respectively). River flow and surface chlorophyll-a were also negatively correlated at WT5.1 (Figure 16; $r^2 = 0.18$), suggesting that flow reduces algal biomass accumulation through either flushing or enhanced turbidity.

Tidal Water Quality comparisons Back River WT4.1 and Patapsco River WT5.1

We revisited the long-term records of nutrient and chlorophyll-a concentrations collected at the sentinel monitoring stations in both the Back and Patapsco estuaries (WT4.1, WT5.1, respectively) to evaluate the potential reversal of water quality improvements in the wake of reported failures at the Back and Patapsco WWTPs. Although the exact timing of these failures is uncertain at this time, it is likely that they began in the fall of 2020 and continued to some extent into 2022. Ross et al. (2022) sampled a station near the discharge of the Patapsco River WWTP in April 2021, and nutrient concentrations and organic wastewater tracers measured there suggested relatively untreated sewage, revealing that failures were occurring at that time. We otherwise relied on the long-term monitoring stations for these analyses to avoid bias that could have emerged if we tried to examine locations in other regions of the estuaries that may have different baseline nutrient levels. This analysis, though simple and limited to March of 2022, revealed a small number of changes in 2022 that might suggest a temporary degradation in water quality. First, summer surface chlorophyll-a concentrations increased at WT5.1 in 2021 to levels that had not been seen in the previous 7 years, and a comparable increase was not observed in the adjacent mainstem Bay (Figure 11). However, both total and dissolved N and P concentration did not remarkably change through spring 2022 at either station relative to recent concentration levels (Figures 17&18).

Sediment Flux Model

While long-term records of water-column nutrient and chlorophyll-a concentrations and their response to eutrophication are common, few long-term records of sediment nutrient release to the water column are available (Boynton et al. 2017). Measurements of sediment-water nutrient and oxygen exchanges are particularly important in relatively shallow systems like Chesapeake Bay and its tributaries because the consumption of oxygen (DO) and release of nitrogen (N), phosphorus (P), and silica (Si) compounds at the sediment-water interface have a strong effect on water quality. In much deeper systems (>20 m) the influence of sediment processes is muted and most DO consumption and nutrient re-cycling occurs in the water column (Boynton et al. 2017). Long-term model simulations suggest that despite a modest reduction in summer water-column chlorophyll-a concentration, modeled sediment-water NH_4 and PO_4 fluxes did not show any substantial declines over time (Figure 19), and the peak modeled rates were relatively high (300 μmol N m^{-2} hr^{-1}, 30 μmol P m^{-2} hr^{-1}). Our baseline simulation in the middle region of the Patapsco Estuary included overlying conditions as measured at station WT5.1, which include persistent near-anoxic throughout June to August. The effect of these low oxygen conditions serves to amplify sediment-water NH_4 and PO_4 fluxes, and we ran additional simulations where bottom water oxygen did not go lower than 2 mg/L to test the impact of hypoxia on the sediment N and P release. The “no-hypoxia” scenarios resulted in a reduction in NH_4 fluxes, where summer peaks were closer to 150 μmol N m^{-2} hr^{-1} and PO_4 fluxes were reduced by 50% (simulations not shown). Finally, we increased the depositional fluxes of carbon, nitrogen, and phosphorus to generate sediment-water NH_4 and PO_4 fluxes that matched those observed at stations in the inner harbor in the mid-1990s (Figure 1) and found that fluxes were 10 times as high in the inner harbor than the lower reaches of the Patapsco estuary. We used these model simulations to inform the nutrient budget exercise.

Nutrient Budget

We synthesized the loading, concentration, and model simulation data collated and generated during this analysis to generate whole-system nitrogen (N) and phosphorus (P) budgets for the Patapsco estuary (Figure 20). We constructed budgets for distinct periods since 1985, including 1985-1990 when industrial and municipal wastewater inputs were large (Figure 3&5), 2010-2014 when wastewater inputs from industrial sources had declined substantially, and for 2019-2020 following upgrades to both the Patapsco and Cox Creek municipal facilities (Figure 4). These computations generated several useful results. First, for nitrogen, where we were able to obtain two estimates of the net exchange of TN between the Patapsco and Chesapeake Bay, the budget had a residual, missing input that was 10-20% of the total loss term (Figure 20). Although some of this “missing” N is associated with error in our budget estimates (e.g., the standard deviation of the box-model N exchange terms was comparable to the mean estimate), we have relatively high confidence in our budget terms, which are highly constrained by observations. The box-model-computed N export term suggested that 78% of imported N was exported to Chesapeake Bay in 1985-1990, 38% in 2010-2014, and 28% in 2019-2020. The overall magnitude of this N export term was reduced from 4.7 10^6 kg/yr in 1985-1990 to 0.6 10^6 kg/yr in 2019-2020, thus wastewater load reductions in the Patapsco resulted in an 87% reduction in N export to Chesapeake Bay. This rapid reduction in N export to the Chesapeake Bay with wastewater upgrades was possible because sediment N recycling was only 12-48% of external loads and denitrification removed 36-63% of the load (Figure 20). In contrast, TP export to Chesapeake Bay either exceeded watershed inputs (as in 1985-1990) or was ~90% of the watershed input (Figure 20). The budget analysis suggests that sediment P recycling supported this P export, as sediment-water P fluxes were 2-4 times higher than the external load, more than enough to compensate for the fact that P burial removed 68-116% of the external load (Figure 20). However, it should be noted that the TP export estimated from the box model was reduced from 0.21 10^6 kg/yr in 1985-1990 to 0.084 10^6 kg/yr in 2010-2014 and to -0.06 in 2019-2020, indicating a decline in TP export to Chesapeake Bay as the external load declined (Figure 20). For both N and P, sediment particulate stocks were the largest terms in the budget, suggesting a substantial reservoir of N and P in the system, one whose reactivity is poorly understood.

Discussion and Conclusions

Estuarine ecosystem responses to mitigation efforts aimed at reversing eutrophication have varied widely, reflecting the fact that internal processes may delay or enhance eutrophication (Duarte et al. 2009), while external forcing (e.g., precipitation, warming) may confound expected nutrient-induced changes (Ni et al. 2020). Prior reports have suggested that eutrophication reversal may be delayed by legacy impacts to sediment communities (Turner et al. 2008; Walve et al. 2018), while in estuaries with long residence times, eutrophication-induced nutrient recycling has the potential to induce positive feedbacks that maintain eutrophication (Savchuk 2018; Testa and Kemp 2012). In contrast to these examples, estuaries where nutrient load reductions were substantial and residence times were fairly low have demonstrated relatively rapid reductions in eutrophication with nutrient load reductions without substantial time delays (Carstensen et al. 2006; Greening and Janicki 2006; Taylor et al. 2020). Our analysis of the Patapsco River estuary suggests it lies somewhere in between these two extremes, where nutrient and chlorophyll-a concentrations declined rapidly and nitrogen export to the mainstem Bay declined in tandem with point source load reductions, but measures of sediment-water recycling and metabolism appear to be relatively unchanged, leading to sustained phosphorus recycling and export. Our discovery that the Patpasco appears to be importing algal biomass from the mainstem Bay is a surprising result that suggests the mainstem may be contributing to oxygen depletion and nutrient recycling in the Patapsco estuary. More advanced spatial monitoring and numerical modeling are required to better quantify the hypothesized mechanisms behind these temporal patterns.

It is clear from our analysis that reductions in both municipal and industrial nutrient loads have resulted in measurable reductions in nitrogen loading to this estuarine ecosystem. WWTP load reductions are especially relevant in the Patapsco River estuary, where they historically represented >90% of the total watershed loads of N and P to the ecosystem (based upon Phase 6 Watershed Model estimates of non-point source inputs) and now contribute ~50% of the total loads. WWTP TN loads have declined roughly 90% since 1985, which is larger than 40% decline in TN concentrations in the estuary during the same period. In the two years since ENR was established at the Patapsco WWTP, TN concentrations reached their lowest level recorded since 1985. Clearly, in-estuary properties are tightly connected to WWTP loads and the water column is highly responsive to nutrient load reductions. What is unique among estuaries where wastewater loading reductions have been associated with water quality improvements is the fact that the major nutrient reductions in the Patapsco appear to be associated with industrial sources, not municipal sources. This fact provides room for more water quality improvements if future upgrades at the Patapsco WWTP can be sustained.

Reductions in estuarine nutrient concentrations associated with WWTP nutrient input reductions appeared to have reduced the potential for phytoplankton biomass accumulation in the Patapsco River. Average summer surface chlorophyll-a concentrations declined by 60% over the record and were especially low in 2019 and 2020 (following ENR), which was consistent with an increased tendency for P concentrations to be at levels potentially limiting phytoplankton growth during summer (N concentrations remained non-limiting; data not shown). This pattern of WWTP loads leading to modest reductions in chlorophyll-a has now been observed in a growing number of estuarine ecosystems (Boynton et al. 2014, Stæhr et al. 2017, Kubo et al. 2018, Reimann et al. 2016, Testa et al. 2022), indicating that even in severely enriched systems, eutrophication reversal can occur within the years of load input declines. The fact that these chlorophyll-a declines have occurred despite increases in adjacent Chesapeake Bay supports the notion of a locally-generated eutrophication reduction.

Bottom water chlorophyll-a concentrations, however, showed and entirely different pattern, where chlorophyll-a increased over the record until 2015, was low for several years, and increased in 2021/2022. The fact that chlorophyll-a at WT5.1 was highly correlated with CB3.2

in the mainstem suggests that the Patapsco is importing chlorophyll-a from the mainstem of Chesapeake Bay. Although it is not clear why CB3.2 chlorophyll-a is increasing over the record in both surface and bottom waters, this pattern has been reported previously (Testa et al. 2018) and appears to be driven by winter blooms, which have been observed elsewhere in Chesapeake Bay (Sellner et al. 1991) and have been associated with mixotrophic algae. Regardless of the ultimate cause, this influx of organic matter from the mainstem Bay, even if chlorophyll-a concentrations are only ~20 µg/L, represents a subsidy of oxygen-consuming, nutrient-rich material that should serve to sustain some aspects of eutrophication in the estuary.

The relationship between phosphorus loading and water column concentration was similar to nitrogen, but phosphorus changes over time were more complex. WWTP TP load reductions accomplished in the early 1990s were on the order of 70-80%, and both surface water TP and PO_4 concentrations declined by a comparable amount (~70%), consistent with a strong correlation between total Patapsco TP load and TP concentration (Figure 9). Although bottom water TP at station WT5.1 also declined over time, bottom-water PO_4 was stable over the past 40 years with substantial interannual variability. Similar discrepancies between load reductions and bottom water concentrations for phosphorus have been observed in other systems (e.g., Kubo et al. 2018, Walve et al. 2018, Testa et al. 2022) and these and other authors have cited sustained phosphorus releases from sediments (i.e., internal loading) as a source of P to maintain higher water-column concentrations for several years following load reductions. Our sediment model simulations suggest little change in the sediment-water P fluxes in the estuary over time, with summer rates typically reaching 40 µmol P m^{-2} hr^{-1}, which is high for Chesapeake Bay estuaries (Boynton et al., in review). These high sediment-water fluxes are sustained by persistent low-oxygen conditions during summer (O_2 <1 mg/L or less at WT5.1 and at select MDE monitoring stations, see supporting information), as low oxygen conditions lead to the accumulation of sulfide and the dissolution of iron oxides, both of which lead to desorption of PO_4 from sediments, increasing porewater concentrations and increasing the concentration gradients that support increased fluxes from sediments.

Budget analyses provide further evidence for a sustained, internal source of phosphorus in the Patapsco River estuary. The fact that phosphorus export to Chesapeake Bay was typically > 50% of the watershed input reveals that sediment-water P fluxes, supported by large sediment particulate stocks, have the potential to replace watershed P load reductions and contribute to P export. Because the Patapsco estuary has persistent low oxygen conditions, there will be a persistent force to help mobilize P from sediments (Testa and Kemp 2012). This result suggests that like other historically enriched estuaries with legacy phosphorus loads (Walve et al. 2018, Stæhr et al. 2017), that a longer timeframe is required to deplete P stocks. However, the box-model-computed exchange estimates do indicate that P export to the mainstem Chesapeake Bay declined as WWTP inputs to the estuary declined, suggesting that the Patapsco has become a smaller contributor to overall Bay loads over time. Given the high uncertainty in these box-model based estimates, new analyses of export fluxes from improved water quality models are needed to better contain these values seasonally and inter-annually.

Cross-system analyses provide an opportunity to place the changes we observed in the Patapsco River into the context of other enriched coastal ecosystems. Across Chesapeake Bay tributaries, there is a strong positive relationship between annual TN loads and summer NH_4 sediment-water fluxes (Figure 10; Testa et al. 2022). When using only the observed Patapsco River NH_4 fluxes, it is clear that the amount of NH_4 flux generated relative to an external TN load is consistent with other hypoxic Bay tributaries and the mainstem Bay itself (Figure 10). We can contrast this with the Back River, where sediment-water NH_4 fluxes (a) declined over time with TN load declines, (b) were lower than the hypoxic systems for a given TN load, and (c) declined less rapidly for a given decline in TN load. All of these features are consistent with an oxic system like the Back River having larger rates of denitrification and thus lower NH_4 fluxes, while the hypoxic Patapsco River estuary has more limited denitrification, allowing higher relative NH_4 fluxes and an amplification of NH_4 flux in higher load years because hypoxia reduces denitrification to enhance NH_4 flux.

Although our estimates of ecosystem metabolic properties did not allow us to evaluate long-term trends, the computations did reveal that the metabolic rates estimated for the middle and lower estuary are much lower than the inner harbor, consistent with known persistent algal blooms in that region of the estuary. The negative relationship between chlorophyll-a in the surface and primary production at Masonville Cove and freshwater inflows suggests that high turbidity or flushing rate limit algal growth during high flow periods. This fact has implications for nutrient export, given that if algal biomass is reduced when nutrient load and flow are high, we would expect a high transfer of nutrients from the Patapsco to the mainstem Bay. Future numerical modeling of this process and, perhaps, more temporally-resolved budget calculations (i.e., interannual) would help quantify this association between flow and nutrient export.

A small part of our analysis included an attempt to discern if the recent reported failures at the Back and Patapsco WWTPs resulted in an abrupt reversal of the positive water quality trends in those systems. Although we were limited to a range of data that did not fully capture 2022 (when new reports of WWTP failures emerged) and our quantitative tools (box model, SFM) were restricted to the 1985-2020 period, we can make some tentative conclusions. First, a simple illustration of the time-series of water-column nutrient concentrations does not show a significant increase in either N or P since 2020 in the Back or Patapsco Rivers (Figures 17&18). Secondly, there did appear to be increases in chlorophyll-a in 2021 and part of 2022 in the Patapsco River, and while we cannot definitively associate these increases with WWTP loads, we might expect that a bloom in these recent years could uptake nutrients and mask any effect of the WWTP failure on nutrient concentration increases. Future work could revisit the time series once they have been more complete and once the sewage treatment plants return to normal operation.

Despite the comprehensive nature of our study, we envision several lines of future work that could build from our analysis or improve the confidence in our findings. First, there has been a wealth of new water quality data collected by different organizations in the estuary that cover a much larger coverage of the estuary, including the inner harbor and several of the tributaries of the Patapsco. Our analysis was focused on the sentinel station at WT5.1 and the MDE stations in its vicinity, given our emphasis on long-term patterns, but future work could begin evaluating the patterns and trends in water quality more broadly in the estuary. These types of analyses could identify hotspots of poor water quality or develop linkages between the main body of the Patapsco with its tributaries. Thus we recommend that regular monitoring (monthly to bi-weekly) of surface and bottom nutrient, oxygen, and chlorophyll-a concentrations be instituted (monthly in winter and monthly-bi-weekly during rest of year) via new monitoring efforts or in collaboration with partner organizations. The sample network (12-15 stations) should span the salinity gradient of the estuary, include major tributaries (e.g., Curtis Bay, Bear Creek, and the Inner harbor areas), and be committed to for multiple years (5-10). Secondly, our nutrient budget estimates relied heavily on numerical model simulations that were not satisfactorily constrained by observations. The SFM simulations we used to estimate denitrification, nutrient burial, and nutrient recycling were only validated against two years of summer measurements made two decades ago, and new sediment-water flux measurements and sediment nutrient content would better constrain our models and indicate if sediments have improved over time. This effort should include measurements between May to September, with a minimum program involving one cruise in August (during hypoxia) and one in May (pre-hypoxia). We suggest making measurements at ~12 locations, corresponding to comparable water-monitoring locations along the salinity gradient and major tributaries. Estimated of sediment nutrient burial could be a component of this program. These new data would help refine the estuary's nutrient budget and would be critical in validating the Phase 7 water quality model. The estimates of Bay-Patapsco nutrient exchange were compiled from a prior CBWQSTM simulation that was not calibrated with the new and extensive water quality measurements and was only run through 2010. A new, higher resolution model could provide better exchange measures, an analysis on long-term changes in the estuary associated with nutrient reductions and climate change, and better quantification of spatial and temporal patterns of metabolic rates, sediment-water fluxes, and hypoxia that control water-quality criteria attainment. The intriguing, but preliminary long-term patterns of dissolved oxygen that suggest co-occurring increases in both water temperature and the duration of oxygen < 5 mg/L could be validated and explained by such a model.

In conclusion, a collation of measurements and model simulations spanning nearly four decades indicates that substantial reductions in WWTP N and P loads to the Patapsco River has resulted in relatively rapid and substantial reductions in water-column nutrient concentrations and chlorophyll-a concentrations. However, several metrics of hypoxia have persisted or even increased over the record at a sentinel station, suggesting that factors beyond nutrient loading and local phytoplankton growth are important, such as organic matter import from the mainstem and climate warming. Both of these controls on hypoxia have likely helped sustain high sediment-water N and P fluxes, which will serve to slow the recovery rate from eutrophication. The failures of wastewater treatment at the Patapsco and Back River WWTPs starting in late 2020 do not appear to have dramatically increased N and P concentrations in the estuary, but there is evidence of higher TN, TP, and bottom water chlorophyll in 2021 relative to the preceding few years. The full year of 2022 data (and perhaps 2023) is required to fully evaluate the potential impact of the WWTP failures. Future work should consider modeling the long-term response of the Patapsco River estuary to WWTP load reductions, and should also consider the potential for newly-collected water quality data from Bluewater Baltimore, the ConMon program, and academic researchers to explore the impact of WWTP reductions in regions of the Patapsco outside of the vicinity of WT5.1 and the Key Bridge.

We arrive at the following "Lessons Learned" from our analysis in the Patapsco estuary:

1. The Patapsco estuary exchanges chlorophyll-a with the mainstem deep water, and this creates an additional import of organic matter to the estuary to fuel hypoxia. Careful attention to this exchange will need to be considered in a Phase 7 water quality model in multiple ways, including (a) quantifying nutrient, oxygen, and organic matter exchange between the Patapsco and mainstem Bay in the Main Bay Water Quality Model as it exists, or (b) be explored as part of a high-resolution Patapsco tributary model.

2. There are many new datasets available that represent spatial water-quality conditions and these data could be analyzed to better understand the water quality response of the estuary to wastewater load reductions, as well as to validate the Phase 7 water quality model.

3. Given the negative relationship between freshwater input and surface water chlorophyll-a and metabolism in the Patapsco estuary, any calibration simulations for the Phase 7 water quality model should span a range of dry and wet conditions.

4. Potential scenarios using the Phase 7 water quality model should include the specific (and isolated) impacts of changes in WWTP loads from the three major plants discharging into tidal water, whose loads were reduced at different times during the last 40 years. Additional scenarios should consider climate changes including warming, altered freshwater flow, and sea level rise and these scenarios should consider how climate effects on the mainstem Bay are transferred to the Patapsco.

References

Beck, M. W., J. D. Hagy and M. C. Murrell. 2015. Improving estimates of ecosystem metabolism by reducing effects of tidal advection on dissolved oxygen time series. Limnol. Oceanogr. Methods 13: 731-745.

Boynton, W.R., C.L.S. Hodgkins, C.A. O'Leary, E.M. Bailey, A.R. Bayard, and L.A. Wainger. 2014. Multi-decade Responses of a Tidal Creek System to Nutrient Load Reductions: Mattawoman Creek, Maryland USA. Estuaries and Coasts 37: 111-127.

Boynton, W.R., M.A.C. Ceballos, E.M. Bailey, C.L.S. Hodgkins, J.L. Humphrey, and J.M. Testa. 2017. Oxygen and Nutrient Exchanges at the Sediment-Water Interface: a Global Synthesis and Critique of Estuarine and Coastal Data. Estuaries and Coasts.

Brady, D. C., J. M. Testa, D. M. Di Toro, W. R. Boynton and W. M. Kemp. 2013. Sediment flux modeling: calibration and application for coastal systems. Estuar. Coast. Shelf Sci. 117: 107-124.

Caffrey, J. M. 2004. Factors controlling net ecosystem metabolism in U.S. estuaries. Estuaries 27: 90-101.

Carstensen, J., D. J. Conley, J. H. Andersen and G. Ærtebjerg. 2006. Coastal eutrophication and trend reversal: A Danish case study. Limnol. Oceanogr. 51: 398-408.

Cronin, W. B. and D. W. Pritchard. 1975. Additional statistics on the dimensions of Chesapeake Bay and its tributaries: Cross-section widths and segment volumes per meter depth. (eds.). Baltimore, Maryland.

Duarte, C.M., Conley, D.J., Carstensen, J., Sánchez-Camacho, M. 2009. Return to Neverland: shifting baselines affect eutrophication restoration targets. Estuaries and Coasts 32: 29-36.

Fisher, T. R., R. J. Fox, A. B. Gustafson, E. Koontz, M. Lepori-Bui and J. Lewis. 2021. Localized Water Quality Improvement in the Choptank Estuary, a Tributary of Chesapeake Bay. Estuaries Coasts

Greening, H. and A. Janicki. 2006. Toward reversal of eutrophic conditions in a subtropical estuary: Water quality and seagrass response to nitrogen loading reductions in Tampa Bay, Florida, USA. Environ. Manage. 38: 163-178.

Kubo, A., F. Hashihama, J. Kanda, N. Horimoto-Miyazaki and T. Ishimaru. 2019. Long-term variability of nutrient and dissolved organic matter concentrations in Tokyo Bay between 1989 and 2015. Limnol. Oceanogr. 64: S209-S222.

Murrell, M. C., J. M. Caffrey, D. T. Marcovich, M. W. Beck, B. M. Jarvis and J. D. I. Hagy. 2018. Seasonal oxygen dynamics in a warm temperate estuary: effects of hydrologic variability on measurements of primary production, respiration, and net metabolism. Estuaries Coasts 41: 690-707.

Ni, W., M. Li and J. M. Testa. 2020. Discerning effects of warming, sea level rise and nutrient management on long-term hypoxia trends in Chesapeake Bay. Sci. Total Environ. 737: 139717.

Odum, H. T. and C. M. Hoskin. 1958. Comparative studies of the metabolism of marine waters. Publications of the Institute of Marine Science-University of Texas 5: 16-46.

Riemann, B., J. Carstensen, K. Dahl, H. Fossing, J. W. Hansen, H. H. Jakobsen, et al. 2015. Recovery of Danish coastal ecosystems after reductions in nutrient loading: A holistic ecosystem approach. Estuaries Coasts 39: 82-97.

Ross, C., A. Gibbs, M. Gonsior, C. Hodgkins, J.M Testa and L.H. Harris. 2022. Anne Arundel County Pilot Wastewater Tracer Study.

Savchuk, O. P. 2018. Large-Scale Nutrient Dynamics in the Baltic Sea, 1970–2016. Front. Mar. Sci. 5:

Scavia, D., I. Bertani, J. M. Testa, A. J. Bever, J. D. Blomquist, M. A. M. Friedrichs, et al. 2021. Advancing estuarine ecological forecasts: seasonal hypoxia in Chesapeake Bay. Ecol. Appl. 31: e02384.

Sellner, K. G., R. V. Lacouture, S. J. Cibil, A. Brindley and S. G. Brownlee. 1991. Importance of a winter dinoflagellate-microflagellate bloom in the Patuxent River estuary. Estuar. Coast. Shelf Sci. 32: 27-42.

Stæhr, P.A., J.M. Testa, and J. Carstensen. 2017. Decadal changes in water quality and net productivity of a shallow Danish estuary following significant nutrient reductions. Estuaries and Coasts 40: 63-79.

Taylor, D. I., C. A. Oviatt, A. E. Giblin, J. Tucker, R. J. Diaz and K. Keay. 2020. Wastewater input reductions reverse historic hypereutrophication of Boston Harbor, USA. Ambio 49: 187-196.

Taylor, D.I., Oviatt C.A., Borkman, D.G. 2011. Non-linear responses of a coastal aquatic ecosystem to large decreases in nutrient and organic loadings. Estuaries and Coasts 34: 745-757.

Testa, J. M., W. M. Kemp, W. R. Boynton and J. D. Hagy. 2008. Long-term changes in water quality and productivity in the Patuxent River estuary: 1985 to 2003. Estuaries Coasts 31: 1021-1037.

Testa, J.M. and W.M. Kemp. 2012. Hypoxia-induced shifts in nitrogen and phosphorus cycling in Chesapeake Bay. Limnology and Oceanography 57(3): 835-850.

Testa, J. M., D. C. Brady, D. M. Di Toro, W. R. Boynton, J. C. Cornwell and W. M. Kemp. 2013. Sediment flux modeling: nitrogen, phosphorus and silica cycles. Estuar. Coast. Shelf Sci. 131: 245-263.

Testa, J. M., W. R. Boynton, C. L. S. Hodgkins, A. L. Moore, E. M. Bailey and J. Rambo. 2022. Biogeochemical states, rates, and exchanges exhibit linear responses to large nutrient load reductions in a shallow, eutrophic urban estuary. Limnol. Oceanogr. https://doi.org/10.1002/lno.12037

Thébault, J., T. S. Schraga, J. E. Cloern and E. G. Dunlavey. 2008. Primary production and carrying capacity of former salt ponds after reconnection to San Francisco Bay. Wetlands 28: 841-851.

Turner, R. E., N. N. Rabalais and D. Justic. 2008. Gulf of Mexico hypoxia: Alternate states and a legacy. Environ. Sci. Technol. 42: 2323-2327.

Walve, J., M. Sandberg, U. Larsson and C. Lännergren. 2018. A Baltic Sea estuary as a phosphorus source and sink after drastic load reduction: seasonal and long-term mass balances for the Stockholm inner archipelago for 1968–2015. Biogeosciences 15: 3003-3025.

Tables

Table 1. Sampling stations, variables, and time period of collection of data used in this analysis.

Station ID	***Items Collected***	***Time Collected***
CB3.2	NH_4, NO_{23}, TN, PO_4, TP, Chlorophyll-a	1985-2021
WT4.1	NH_4, NO_{23}, TN, PO_4, TP, Chlorophyll-a	1985-2021
WT5.1	NH_4, NO_{23}, TN, PO_4, TP, Chlorophyll-a	1985-2021
Metabolism		
Aquarium East (AES)	Dissolved Oxygen, Salinity, Temperature	2009-2021
Aquarium West (AWS)	Dissolved Oxygen, Salinity, Temperature	2016-2021
Ft. McHenry (MCH)	Dissolved Oxygen, Salinity, Temperature	2004-2013
Masonville Cove (MSV)	Dissolved Oxygen, Salinity, Temperature	2016-2021
Ft. Armistead (ARM)	Dissolved Oxygen, Salinity, Temperature	2009-2011
Ft. Smallwood (SMA)	Dissolved Oxygen, Salinity, Temperature	2009-2011

Figures

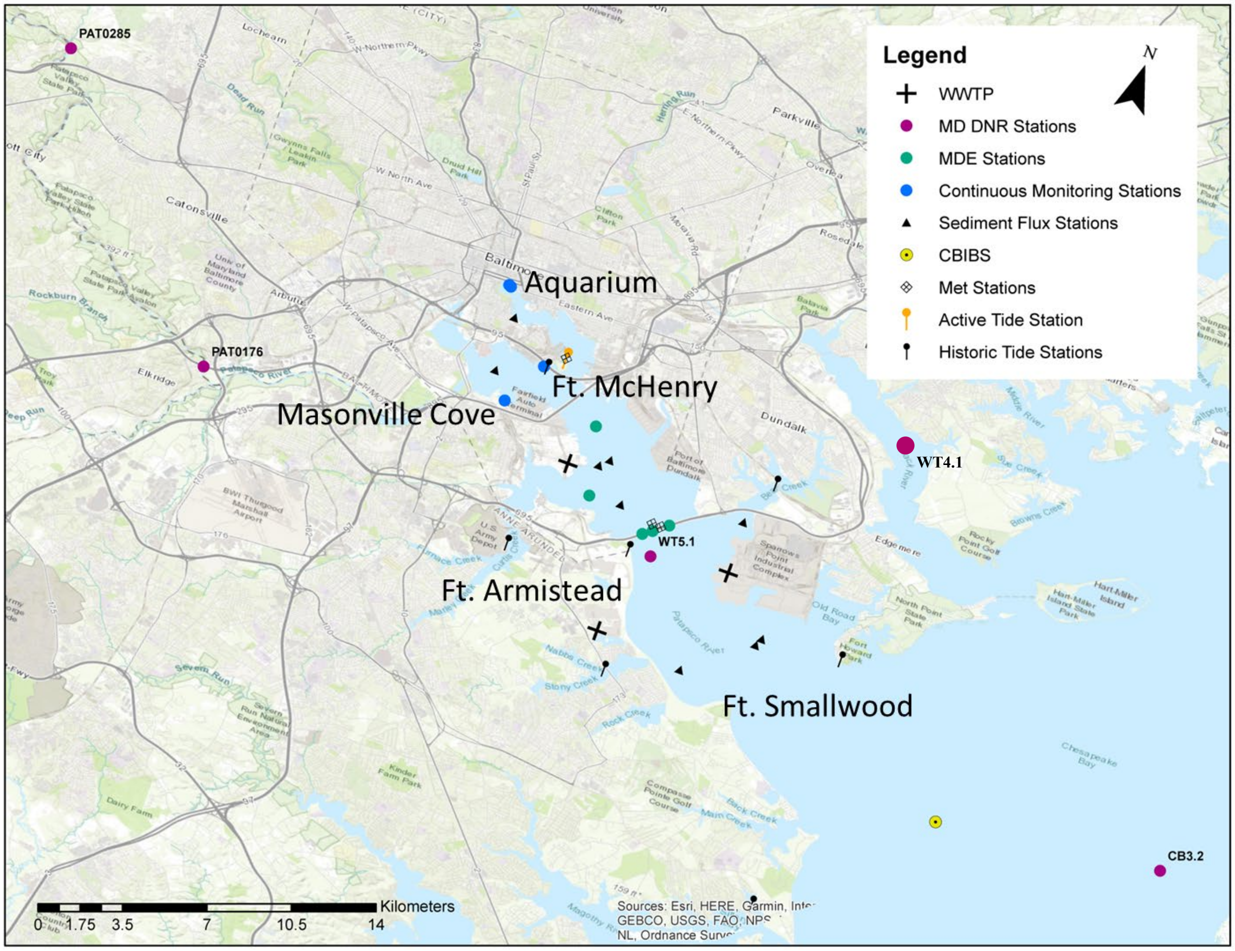

Figure 1: Location of monitoring stations in the Patapsco and Back River estuaries and the nearest mainstem Chesapeake Bay station. Blue circles indicate continuous monitoring stations for dissolved oxygen, temperature, salinity, and chlorophyll-a (also Ft. Armistead and Ft. Smallwood), maroon circles are long-term water quality monitoring stations for dissolved oxygen, chlorophyll-a, nitrogen and phosphorus concentrations, green circles are MDE water quality monitoring stations, triangles are historic sediment-water flux sites, crosses are major WWTPs (W.R. Grace not included), and pins/yellow circles are tide/meteorological stations.

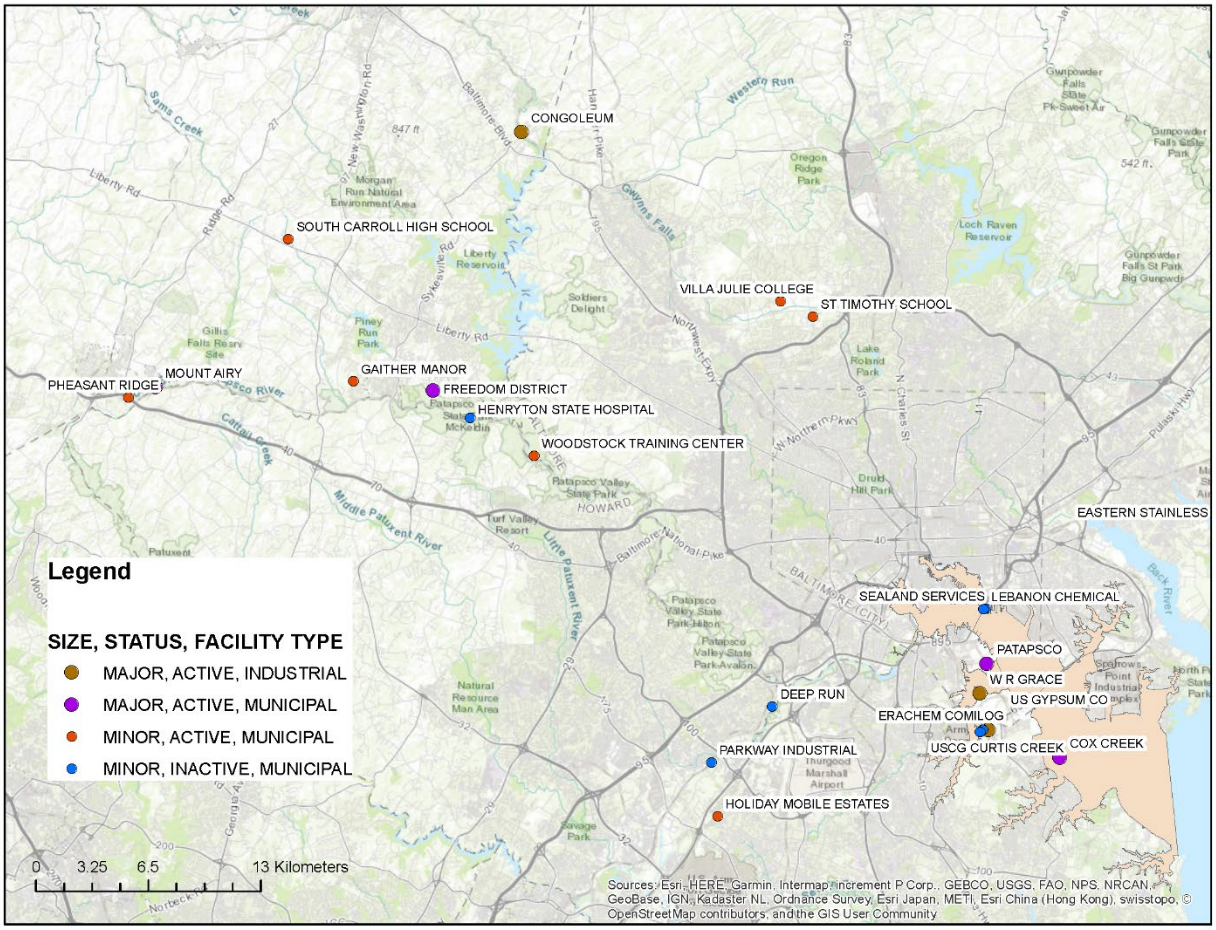

Figure 2: Location of point source facilities in the Patapsco River estuary and watershed, where facilities are colored by size (major, minor), and type (industrial, municipal). Note that these are currently operating facilities, and Sparrows Point is not included, despite its large contribution to nutrient loads over the last four decades.

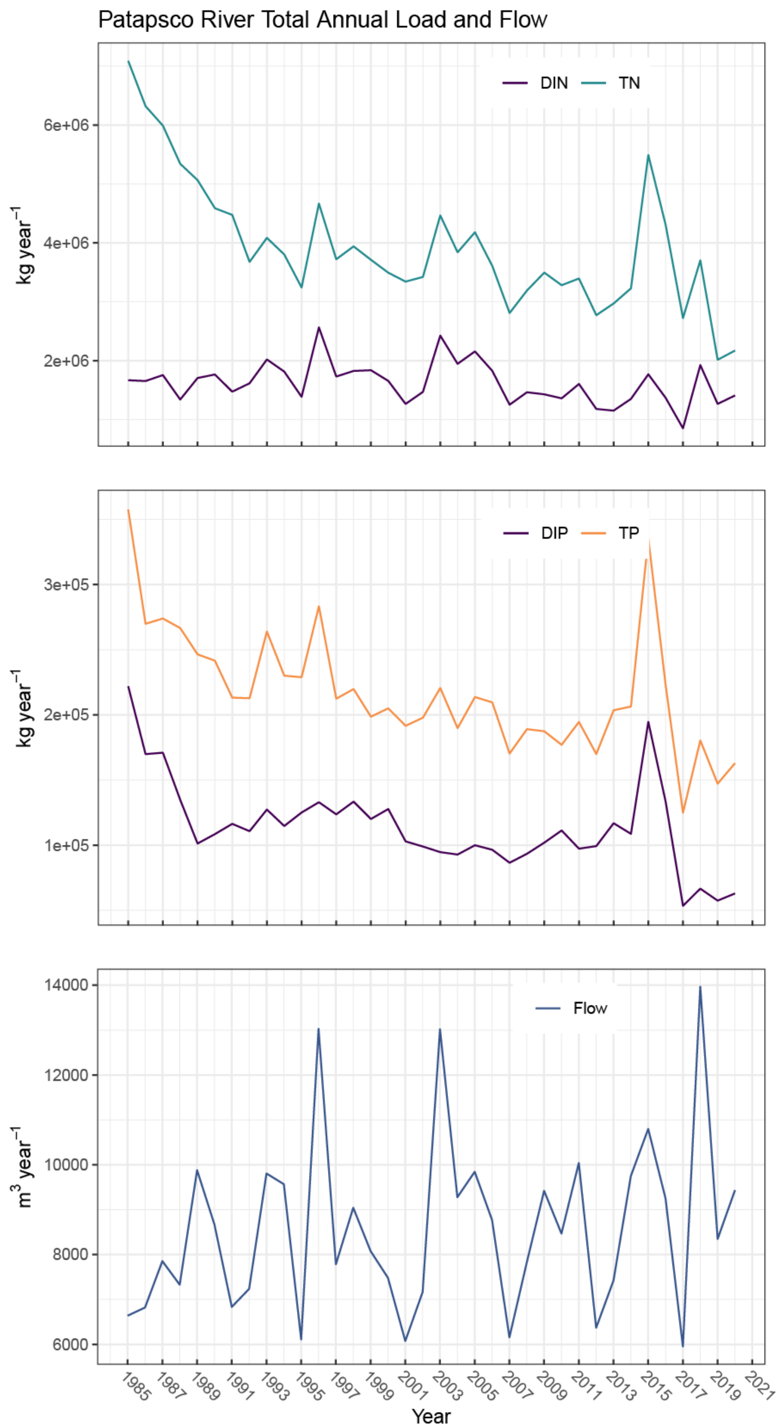

Figure 3: Time-series (1985-2021) of total Patapsco River nitrogen loads (top panel; TN=total nitrogen, DIN = dissolved inorganic nitrogen), phosphorus loads (middle panel; TP=total phosphorus, DIP = dissolved inorganic phosphorus), and total freshwater flow (bottom panel).

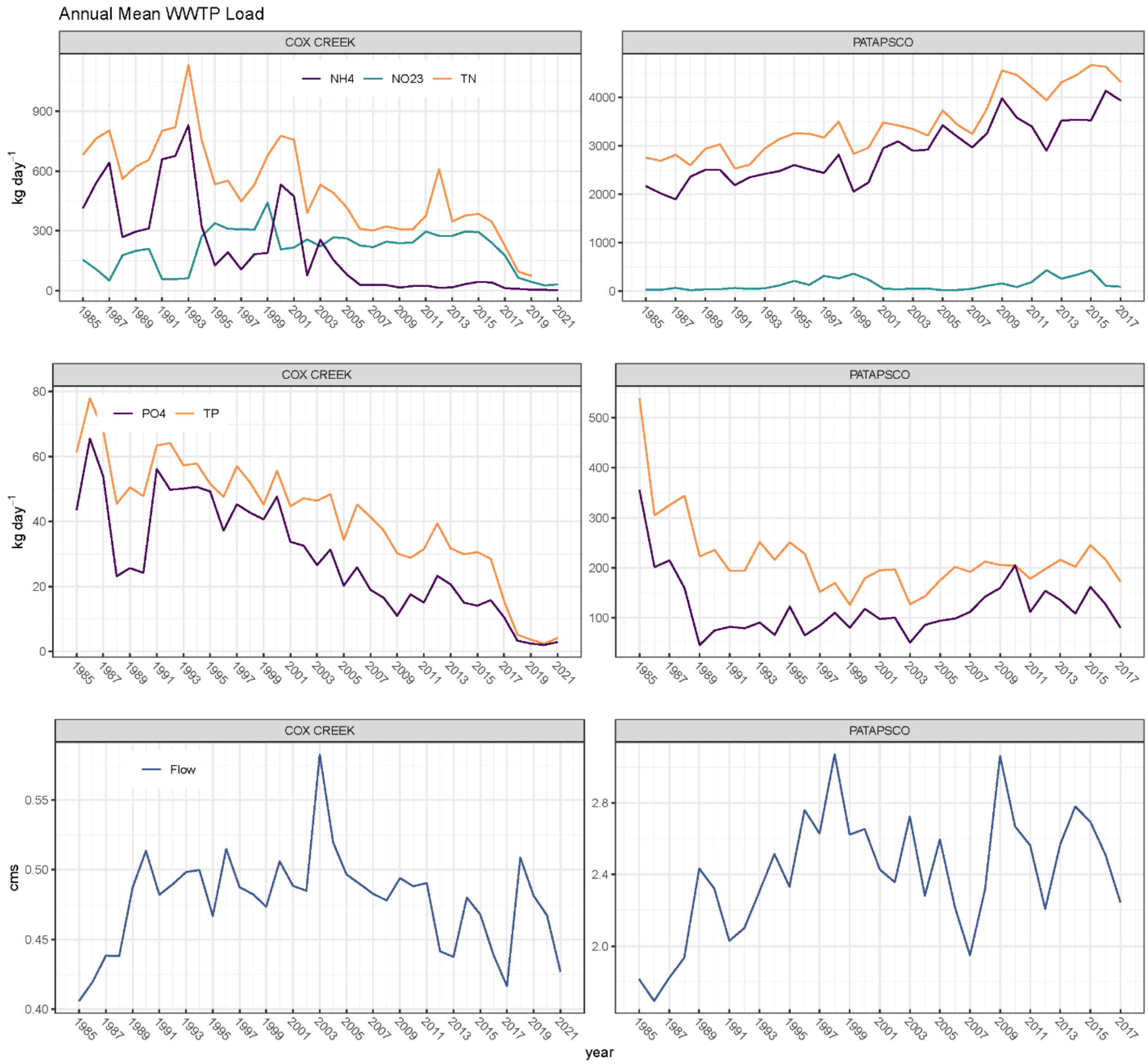

Figure 4: Time-series (1985-2021) of wastewater nutrient and water inputs from two major tidal treatment plants (Cox Creek on left, Patapsco on right), including nitrogen loads (top panels; TN=total nitrogen, NH_4= ammonium, NO_{23} = nitrate plus nitrite), phosphorus loads (middle panels; TP=total phosphorus, PO_4 = dissolved orthophosphate = DIP), and total water discharge (bottom panels).

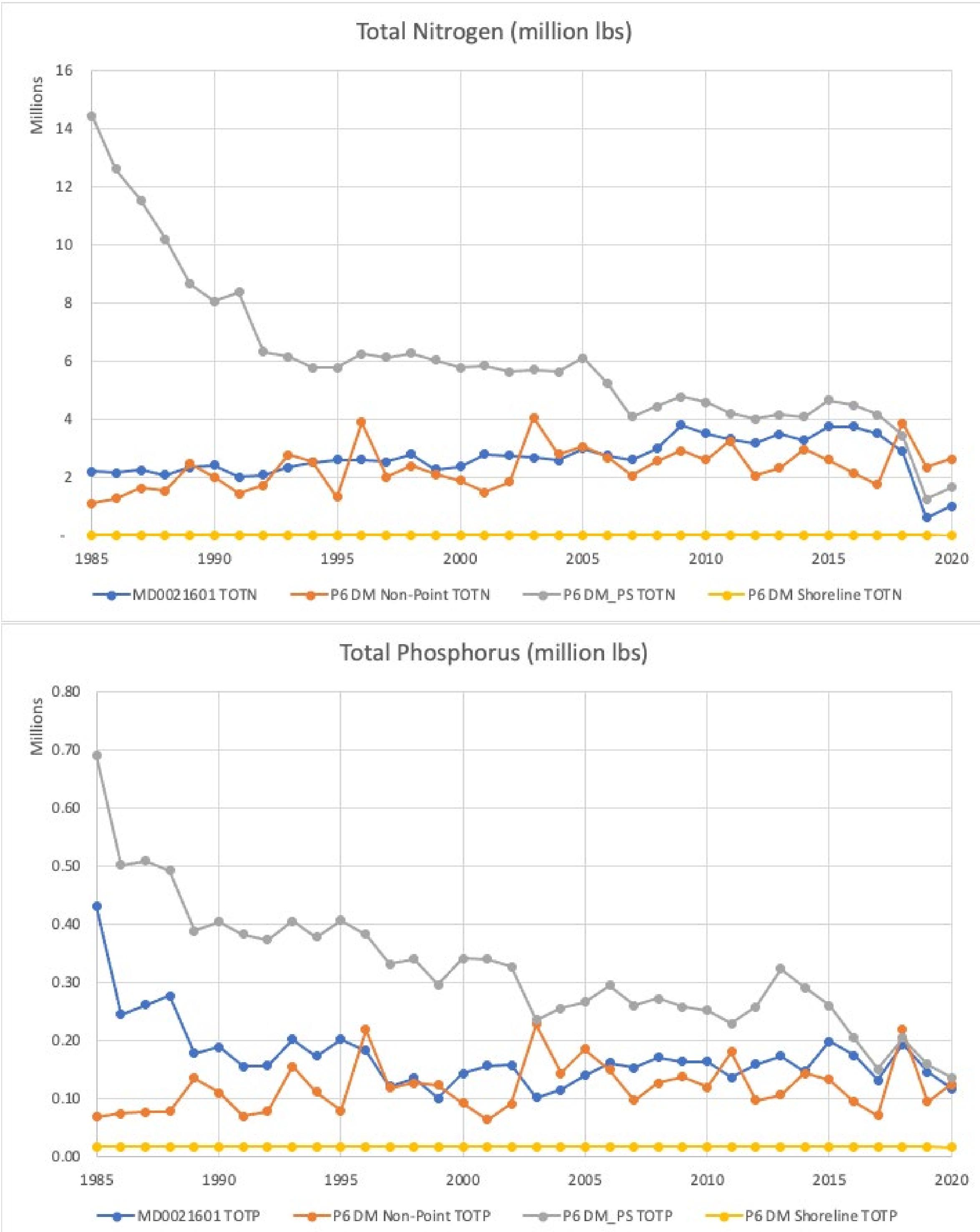

Figure 5: Time-series (1985-2020) of total nitrogen (top panel, TOTN) and phosphorus (bottom panel, TOTP) Phase 6 watershed model loads from all tidal point sources (P6 DM_PS), all non-point sources (P6 DM_Non-Point), and the Patapsco WWTP (MD0021601). Patapsco WWTP loads from NPDES (National Pollutant Discharge Elimination System). Shoreline loads are negligible in the Patapsco estuary.

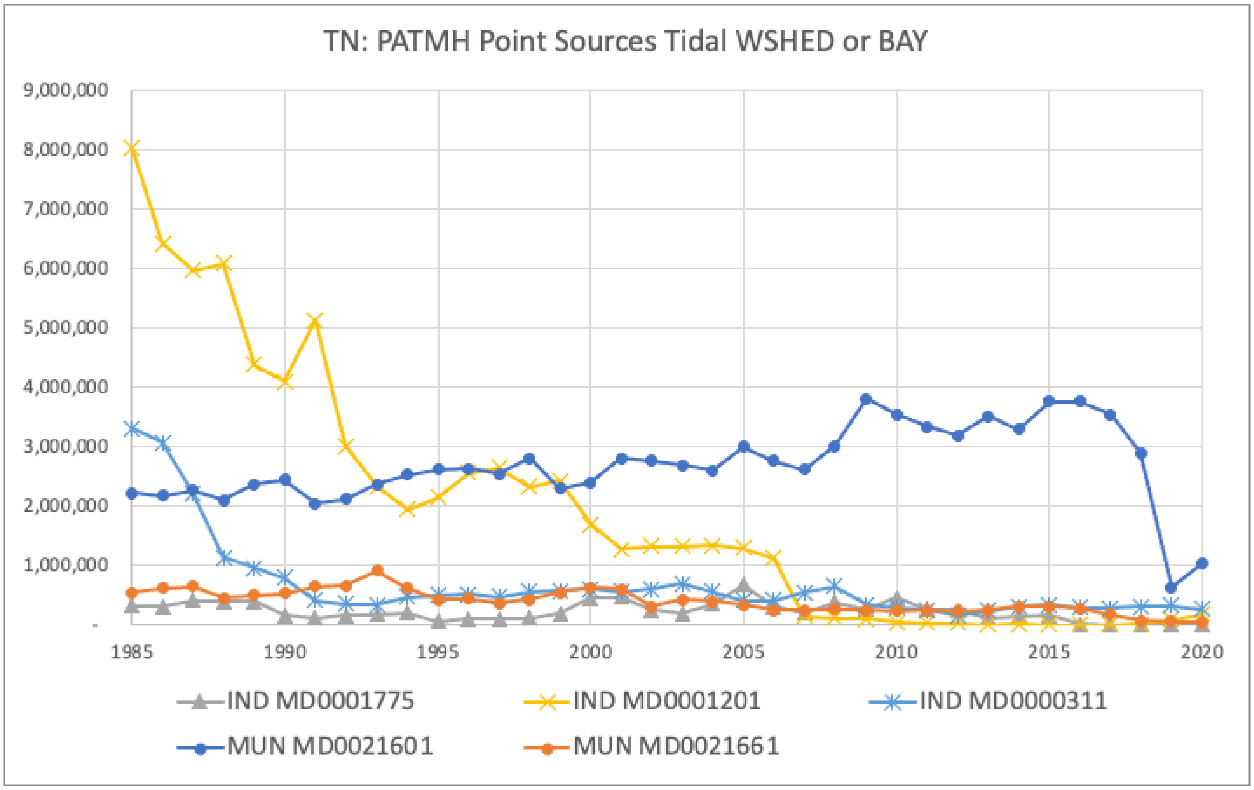

Figure 6: Time-series (1985-2020) of total nitrogen loads from major industrial and municipal tidal point sources, including the Patapsco WWTP (MUN MD0021601), Sparrows Point (IND MD0000311), W.R. Grace (IND MD0001201), and Cox Creek (MUN MD0021661). Loads from NPDES (National Pollutant Discharge Elimination System).

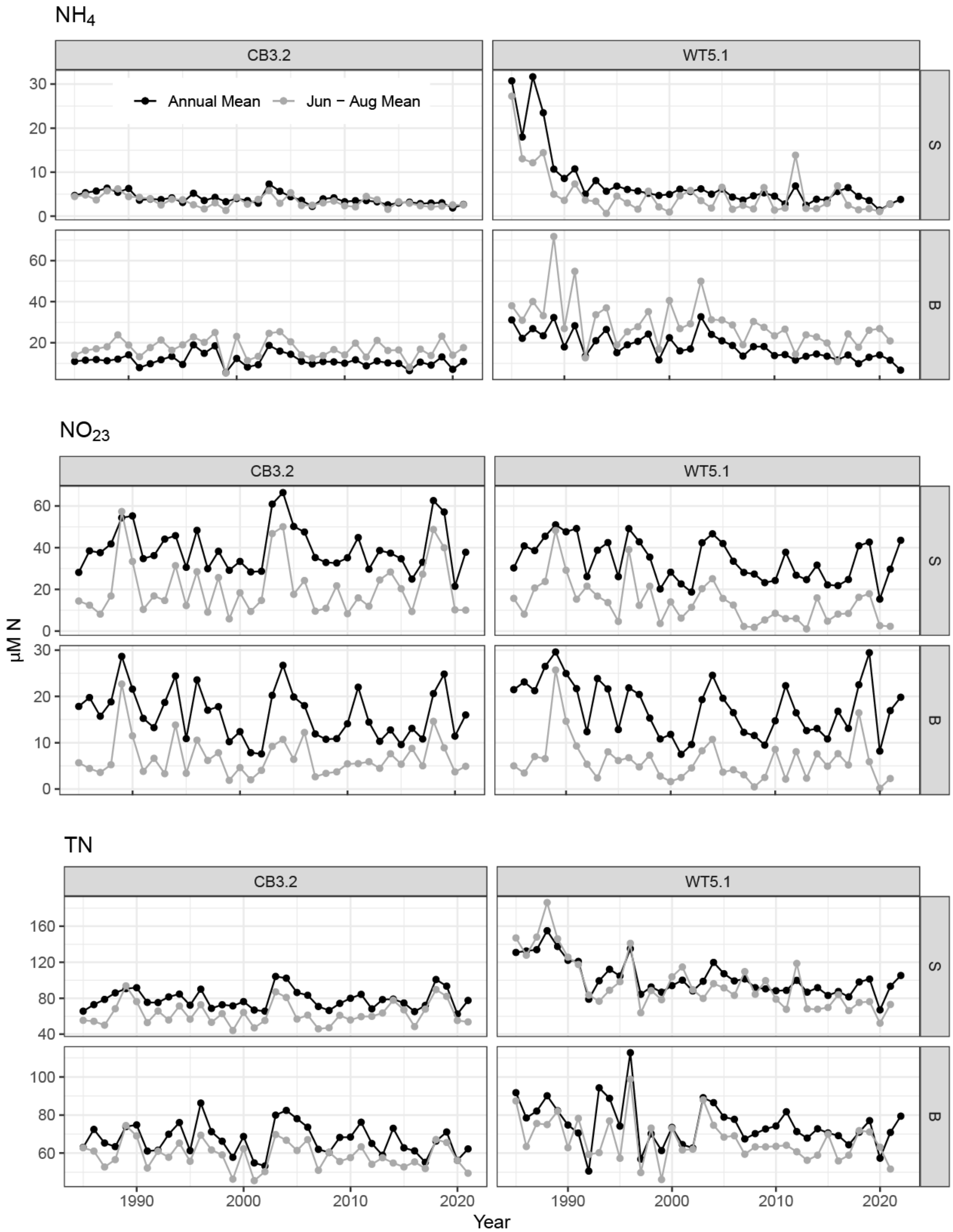

Figure 7: Time-series (1985-2021) of surface (S) and bottom (B) water nutrient concentrations in the Patapsco estuary (WT5.1) and adjacent mainstem Chesapeake Bay (CB3.2), including (top panels) NH_4= ammonium, (middle panels) NO_{23} = nitrate plus nitrite, and (bottom panels) TN=total nitrogen. Dark lines are annual averages and light lines are summer (June to August) averages.

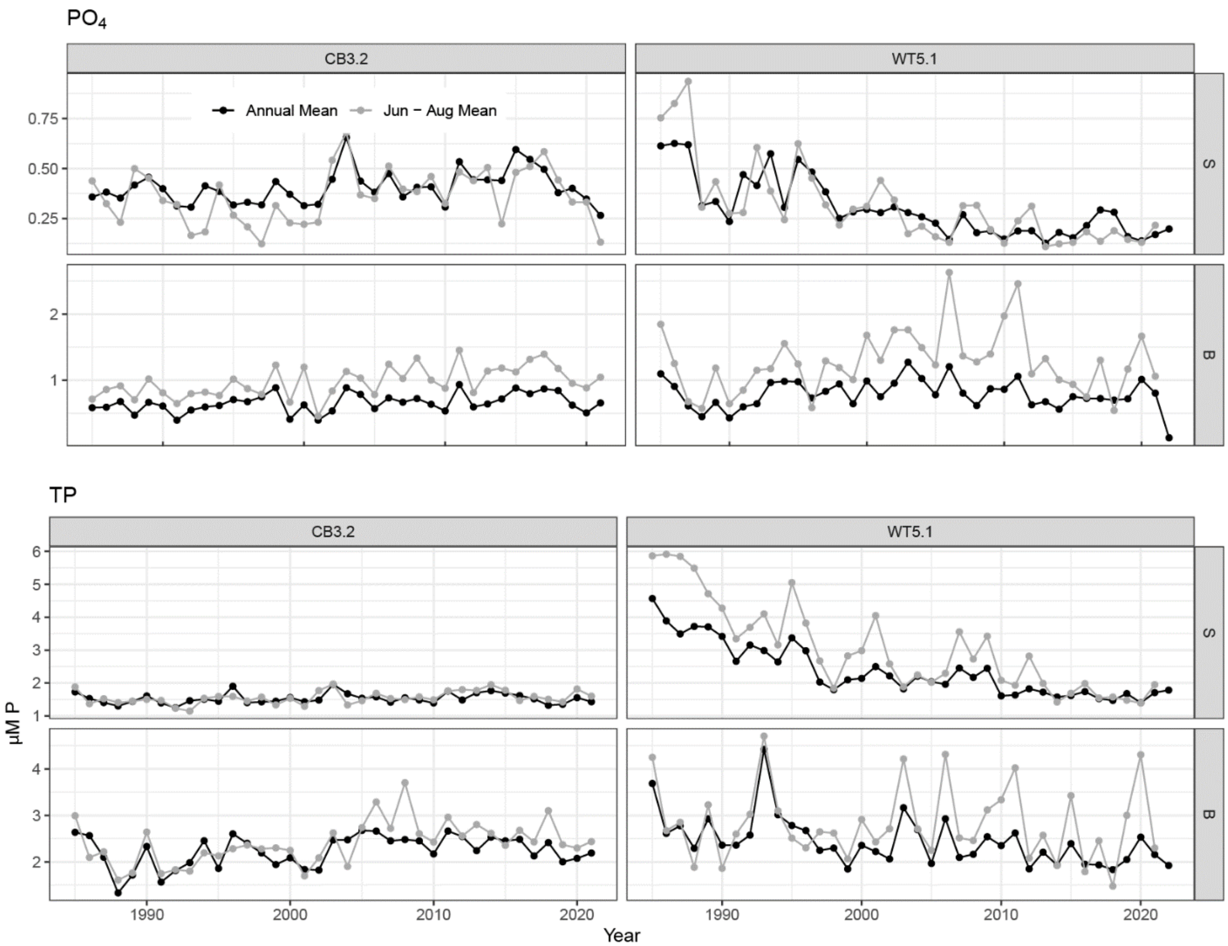

Figure 8: Time-series (1985-2021) of surface (S) and bottom (B) water nutrient concentrations in the Patapsco estuary (WT5.1) and adjacent mainstem Chesapeake Bay (CB3.2), including (top panels) PO_4 = dissolved orthophosphate = DIP and (bottom panels) TP=total phosphorus. Dark lines are annual averages and light lines are summer (June to August) averages.

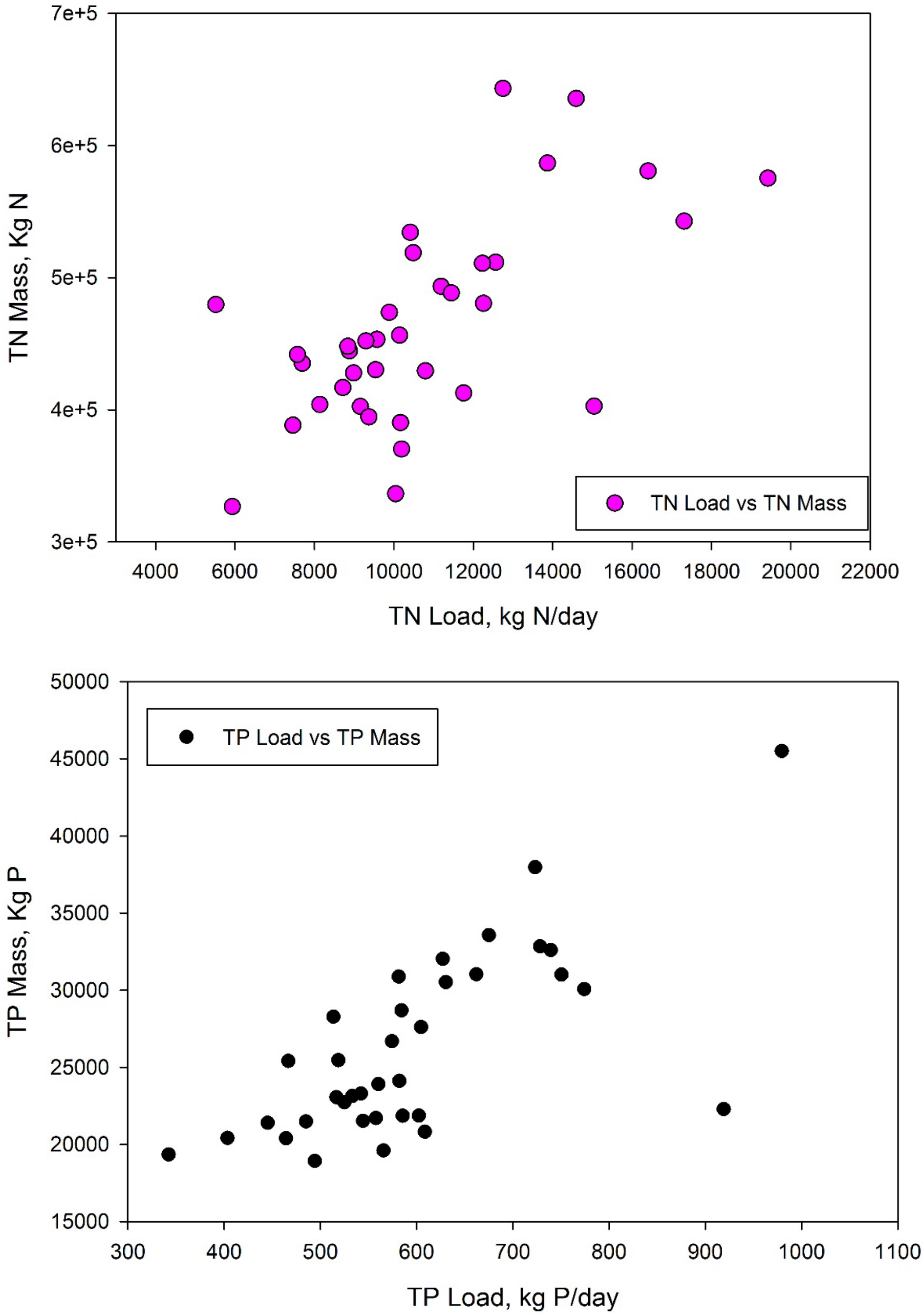

Figure 9: Correlations between total watershed nutrient loads and total estuarine nutrient mass (TN, TP) including annual-scale data from 1985-2021.

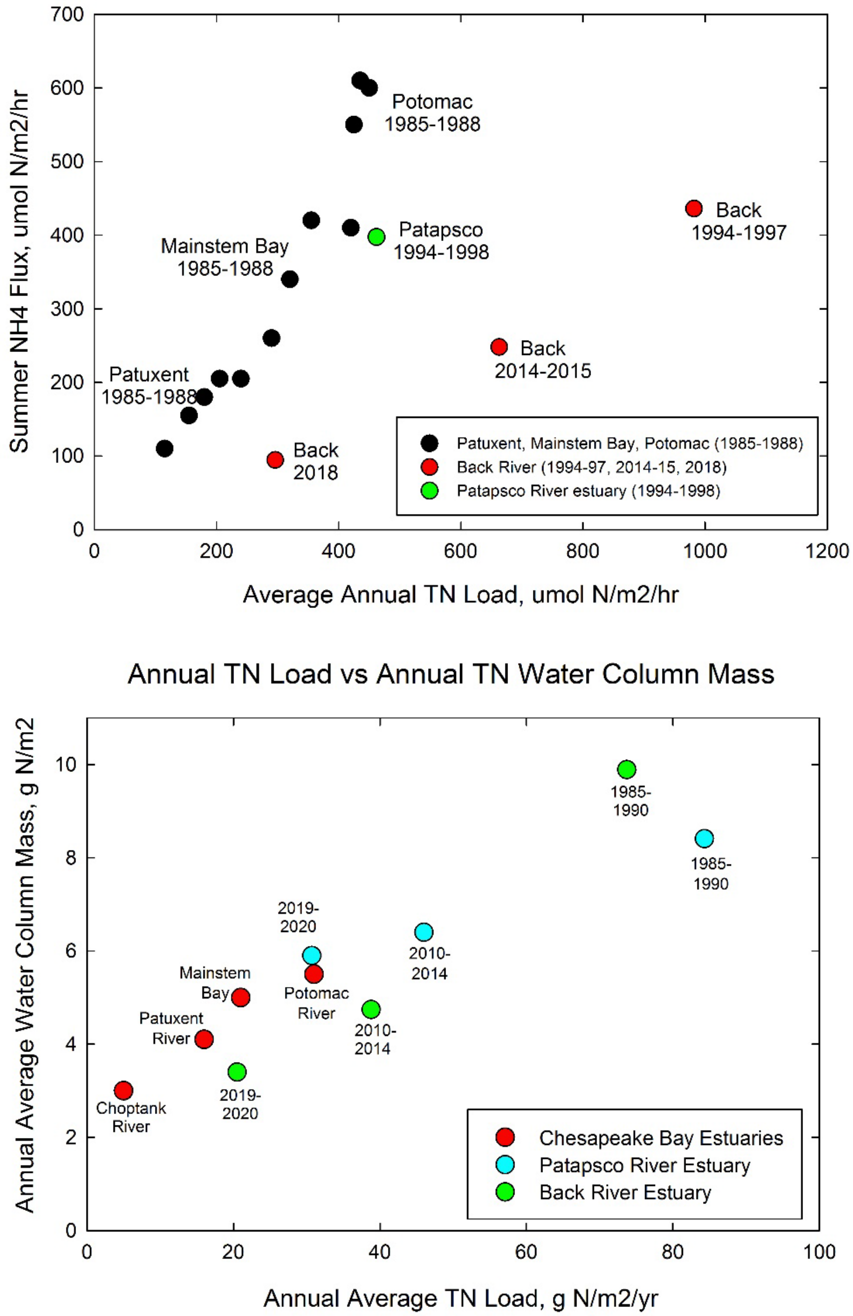

Figure 10: (top panel) Correlations between total annual average total nitrogen (TN) load and summer sediment-water nutrient fluxes across multiple Chesapeake Bay systems, including mainstem Chesapeake Bay, the Patuxent River, the Potomac River (dark circles) and the Back and Patapsco River estuaries where data are available. (bottom panel) Correlations between total annual average total nitrogen (TN) load and total estuarine nutrient mass (TN) in multiple Chesapeake Bay systems, including mainstem Chesapeake Bay, the Patuxent River, the Potomac River, and the Choptank River (red circles) and the Back and Patapsco River estuaries where data are divided by time-periods with different WWTP treatment levels.

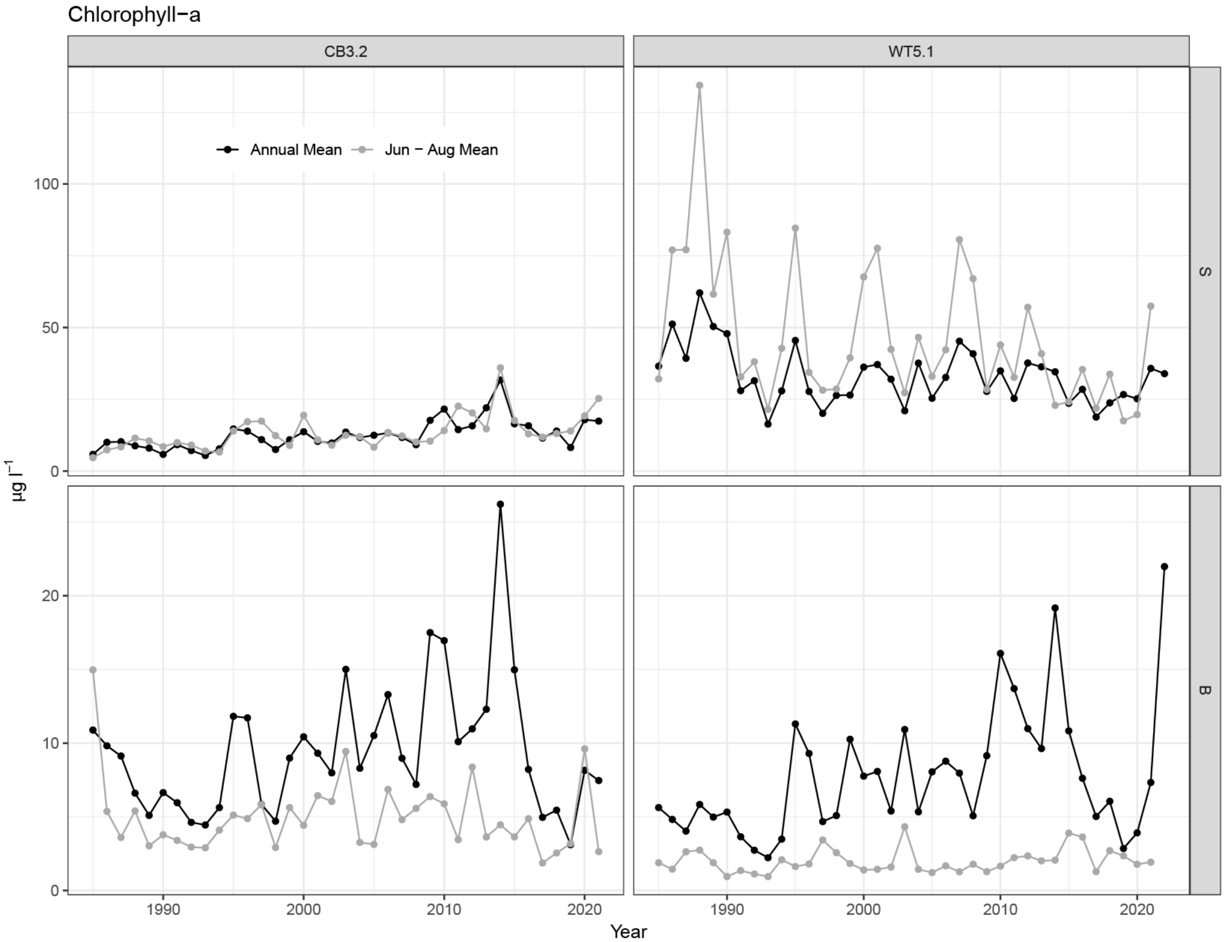

Figure 11: Time-series (1985-2021) of surface (S) and bottom (B) water chlorophyll-*a* concentrations in the Patapsco estuary (WT5.1) and adjacent mainstem Chesapeake Bay (CB3.2).

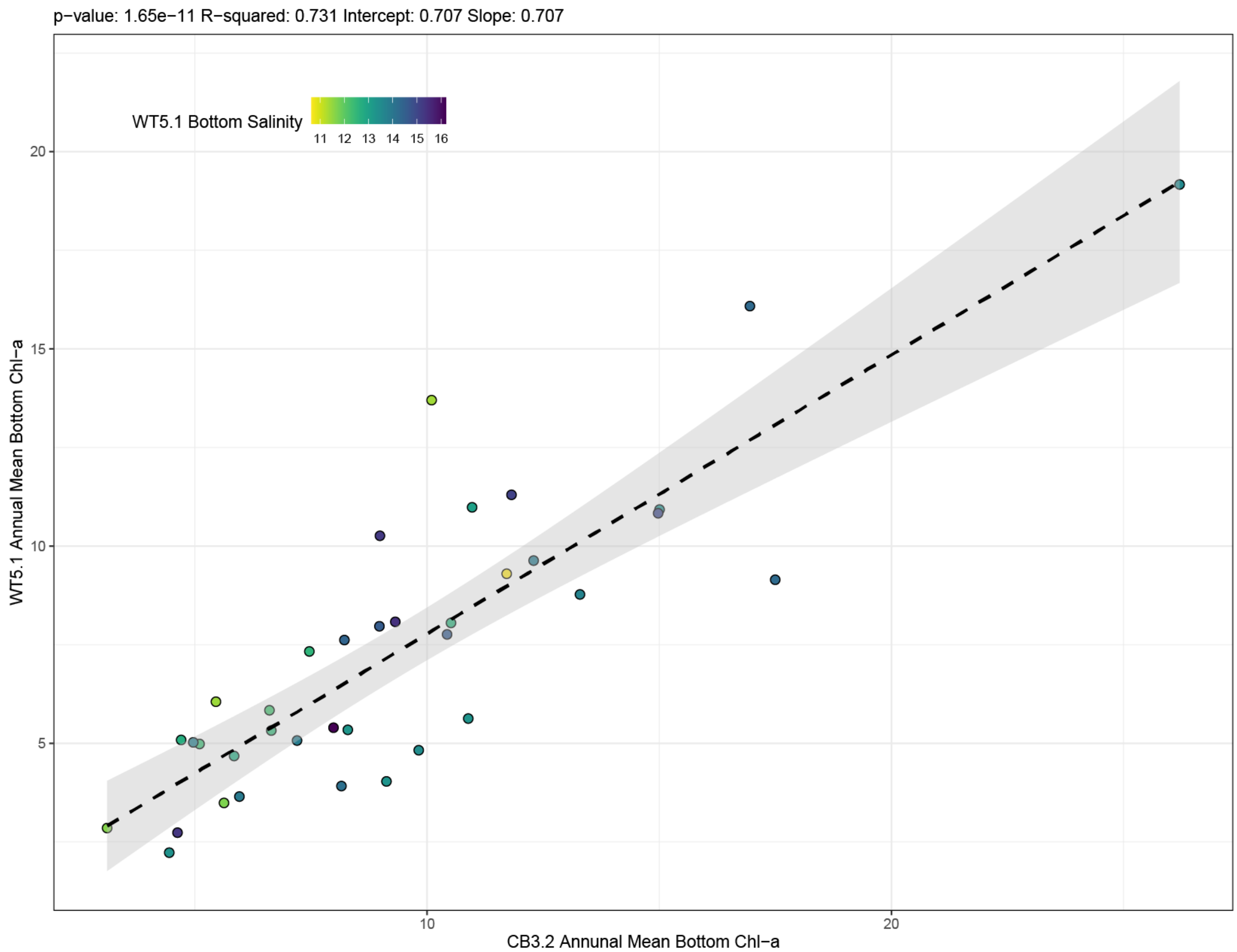

Figure 12: Correlation between annual mean bottom water chlorophyll-*a* concentrations in the Patapsco estuary (WT5.1) and adjacent mainstem Chesapeake Bay (CB3.2).

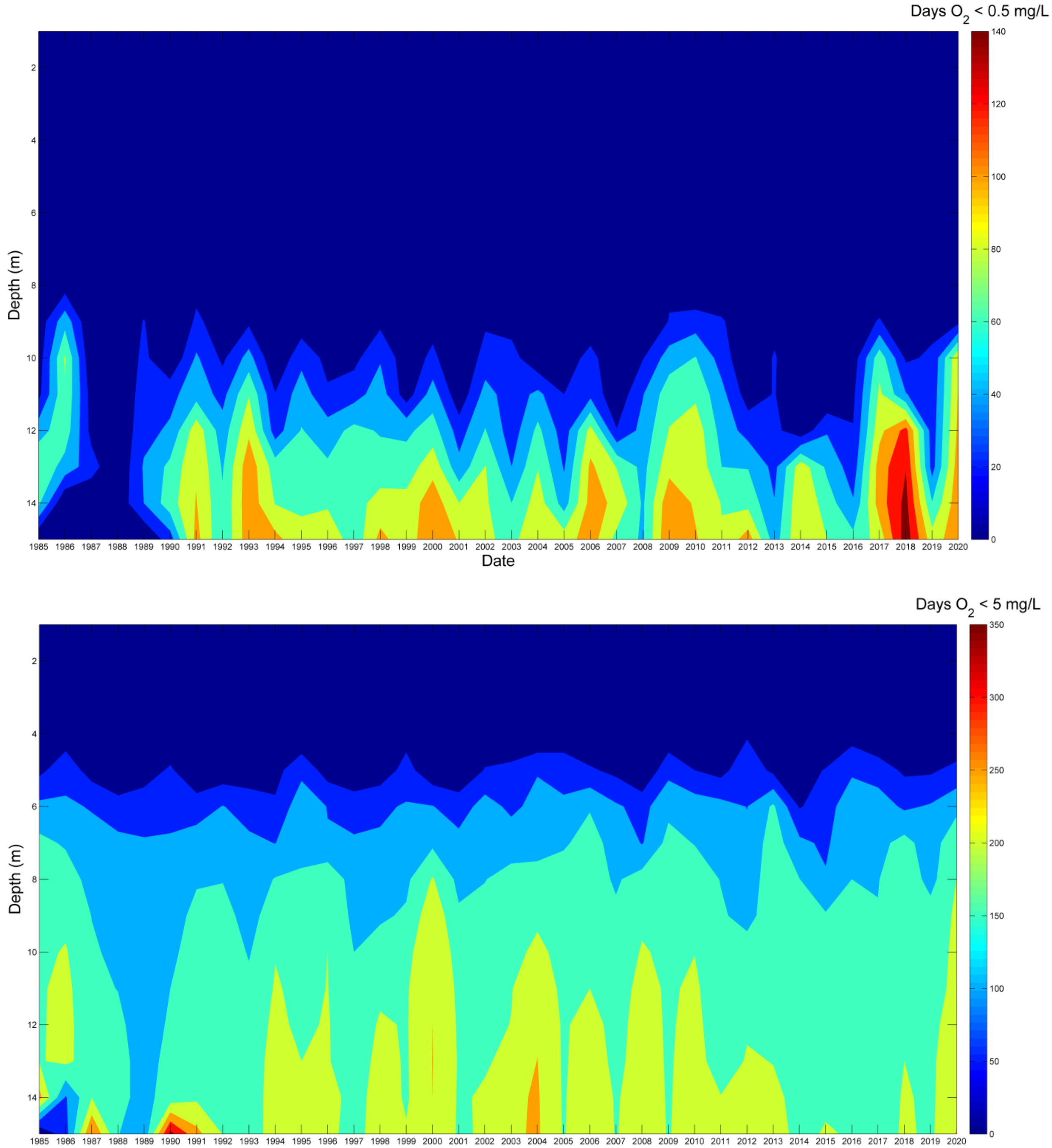

Figure 13: Contour plots representing the number of days in a year that a given depth experiences oxygen concentrations below (top) 0.5 mg/L and (bottom) 5 mg/L over the 1985-2020 period. Computations derived from a linear interpolation to daily values of available oxygen concentrations made at station WT5.1.

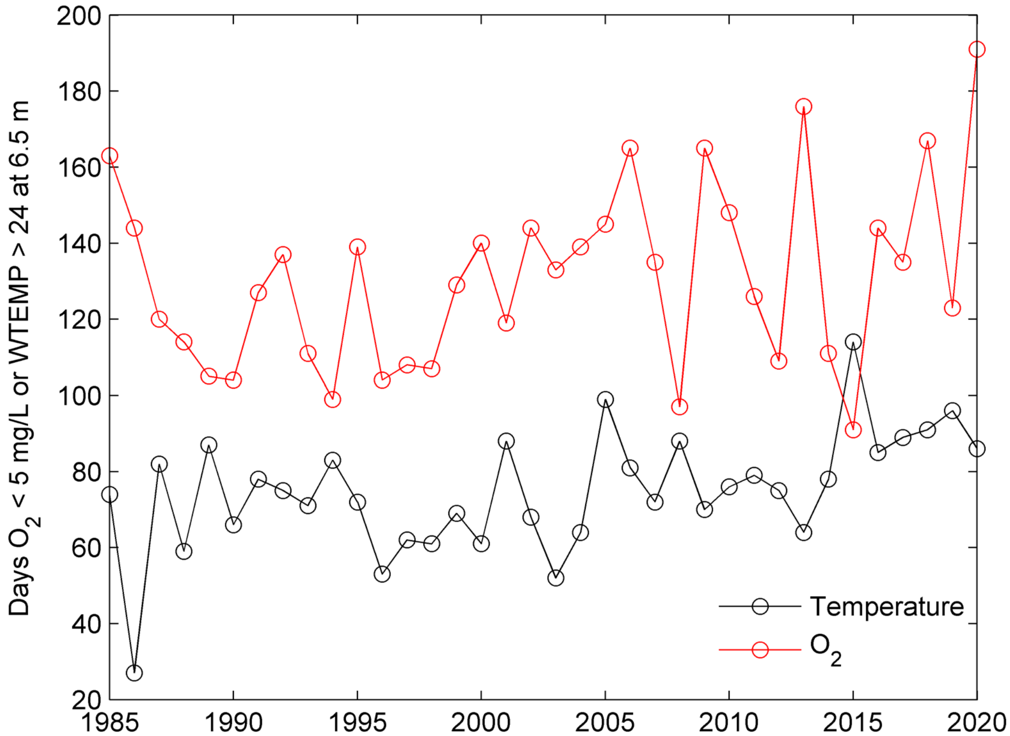

Figure 14: Time series of the annual number of days dissolved oxygen is below 5 mg/L (red line) and water temperature is greater than 24 deg C (black line) over the 1985-2020 period at 6.5 m depth. Computations derived from a linear interpolation to daily values of available oxygen and water temperature concentrations made at station WT5.1.

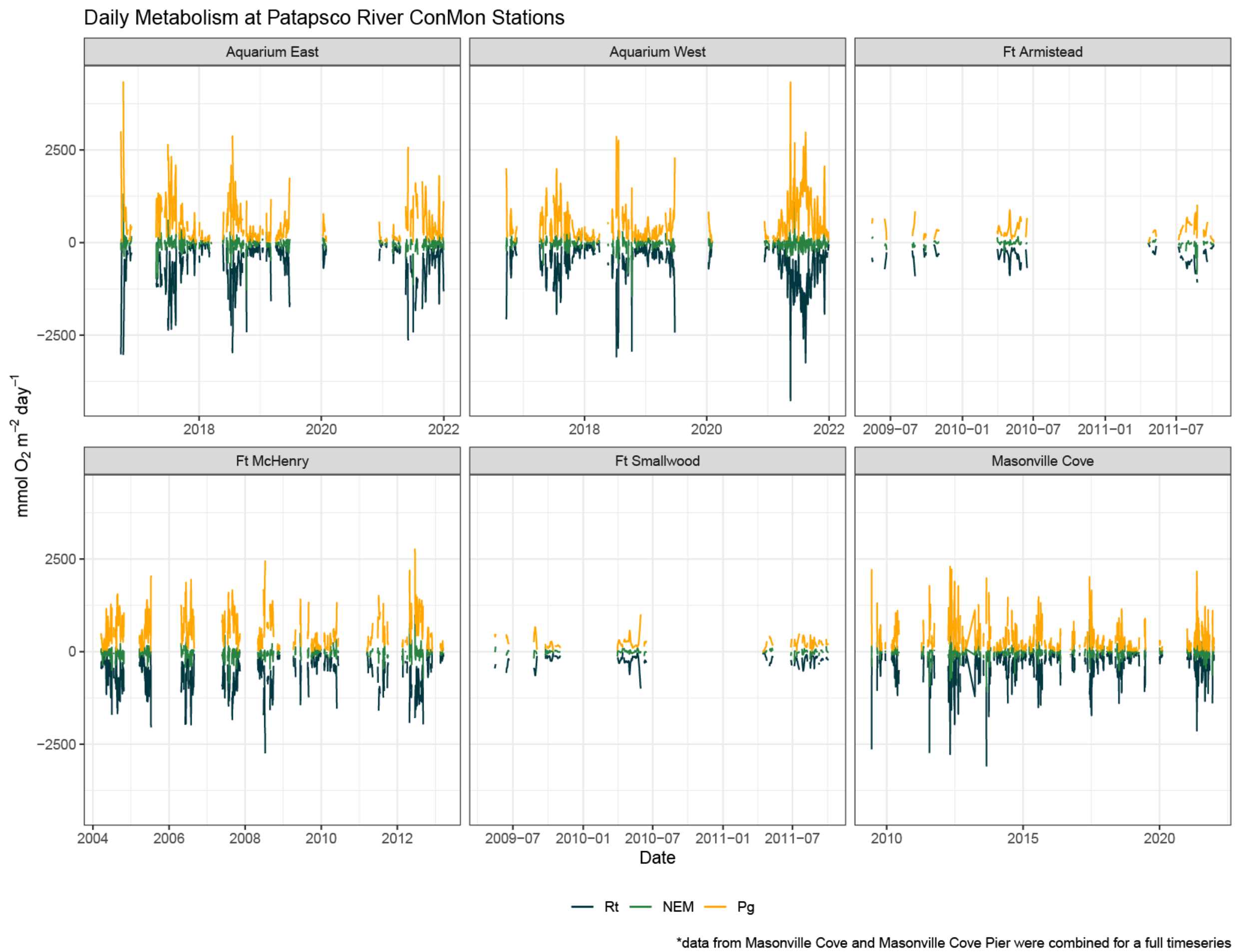

Figure 15: Time-series of daily estimates of metabolic properties derived from high frequency dissolved oxygen sensors from 6 locations in the Patapsco River estuary. Rate estimates include ecosystem respiration (Rt, blue lines), Ecosystem gross primary productivity (Pg, yellow lines), and net ecosystem metabolism (NEM = Pg-Rt, green lines).

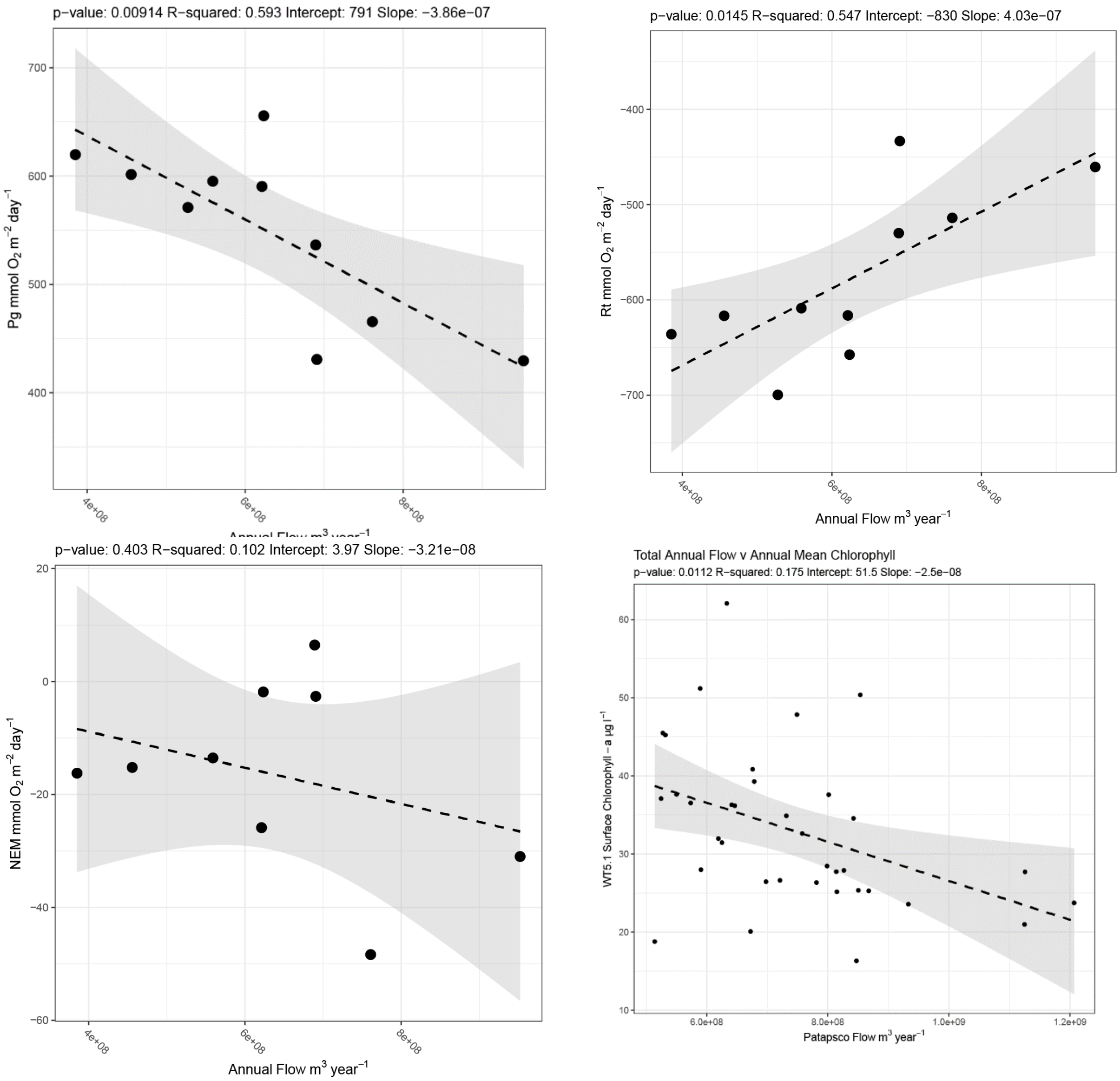

Figure 16: Correlations between annual Patapsco river discharge and various metrics of plankton metabolism, including (top left) summer mean Pg at Masonville Cove, (top right) summer mean Rt at Masonville Cove, (bottom left) summer mean NEM at Masonville Cove, and (bottom right) annual average chlorophyll-*a* at WT5.1.

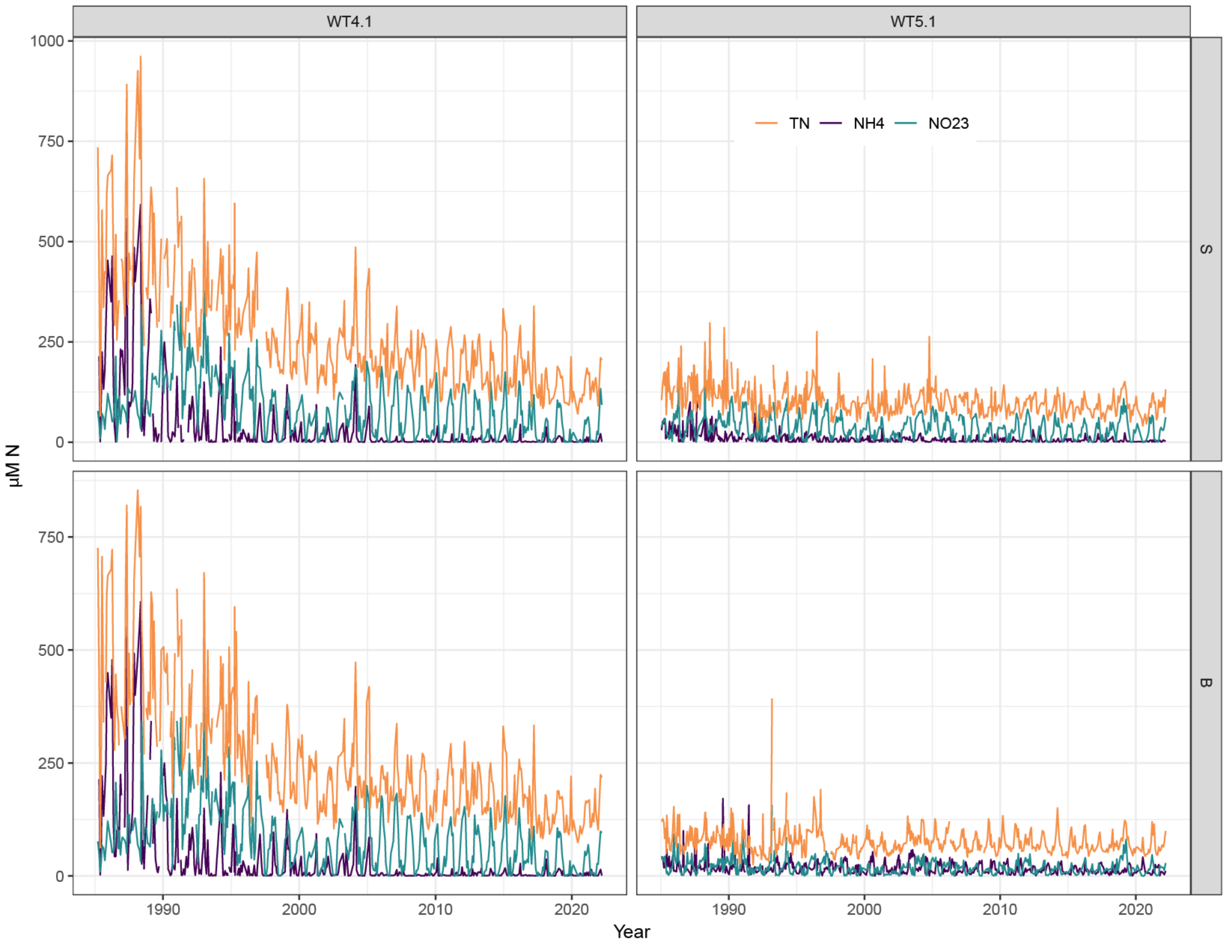

Figure 17: Time-series (1985-March 2022) of surface (S; top panels) and bottom (B; bottom panels) water nutrient concentrations in the Patapsco estuary (WT5.1) and Back River estuary (WT4.1), including NH_4= ammonium, NO_{23} = nitrate plus nitrite, and TN=total nitrogen.

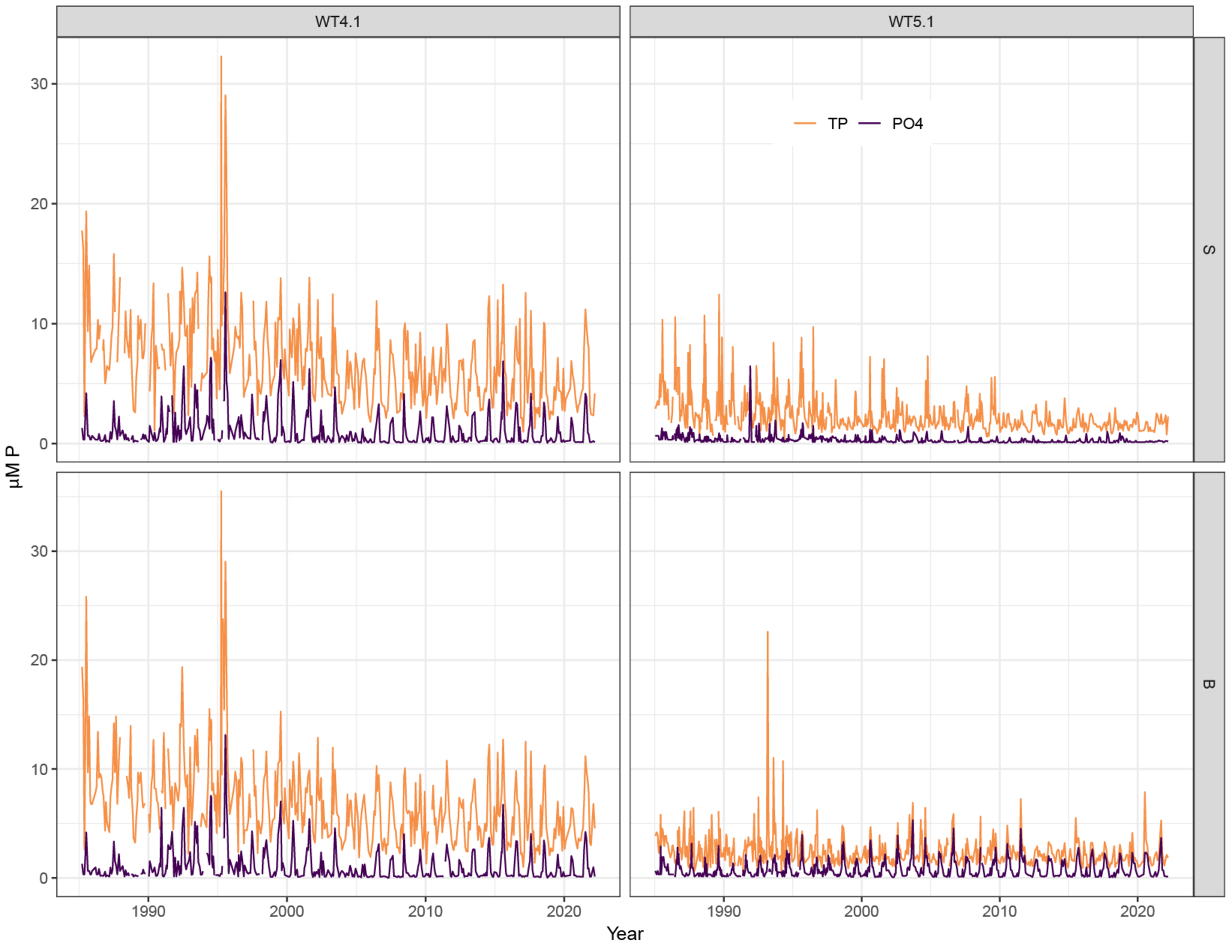

Figure 18: Time-series (1985-March 2022) of surface (S; top panels) and bottom (B; bottom panels) water nutrient concentrations in the Patapsco estuary (WT5.1) and Back River estuary (WT4.1), including PO_4 = dissolved orthophosphate = DIP and TP=total phosphorus.

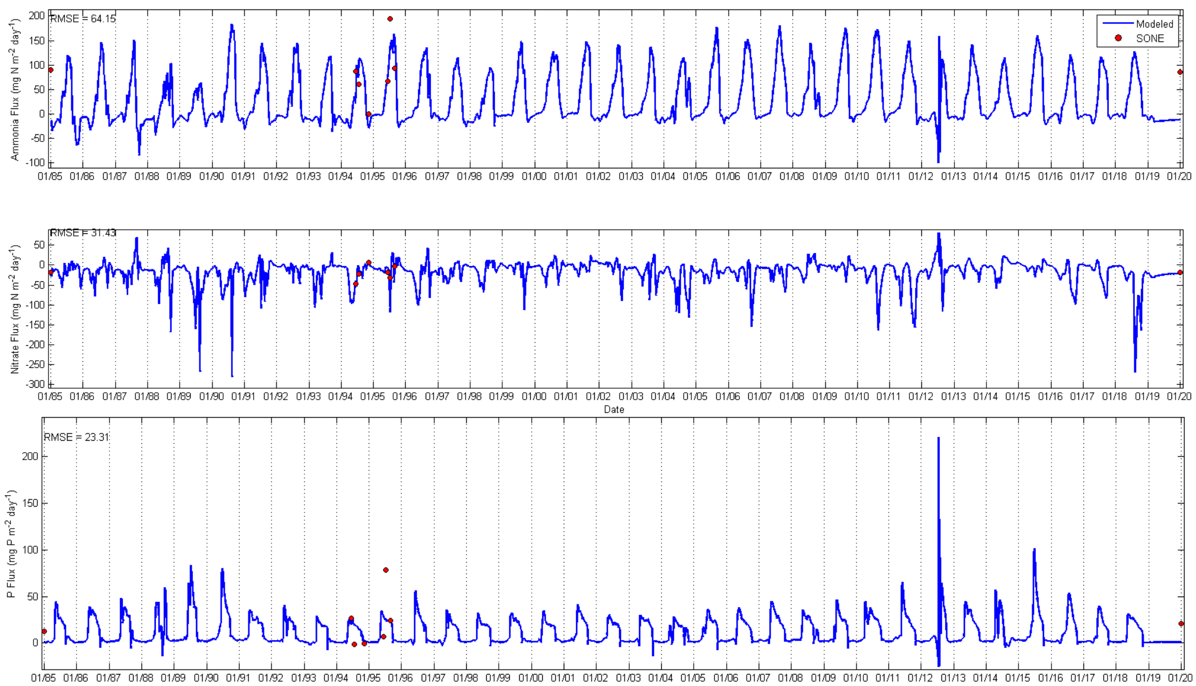

Figure 19: Comparison of measured (red circles) sediment-water fluxes of ammonium (top), nitrate (middle), and phosphate and SFM-simulated (blue lines) daily sediment-water fluxes in the mid-Patapsco estuary over the 1985-2020 period. Note red circles in 1985 and 2020 can be ignored. RMSE = root mean squared error of the model-observation comparison.

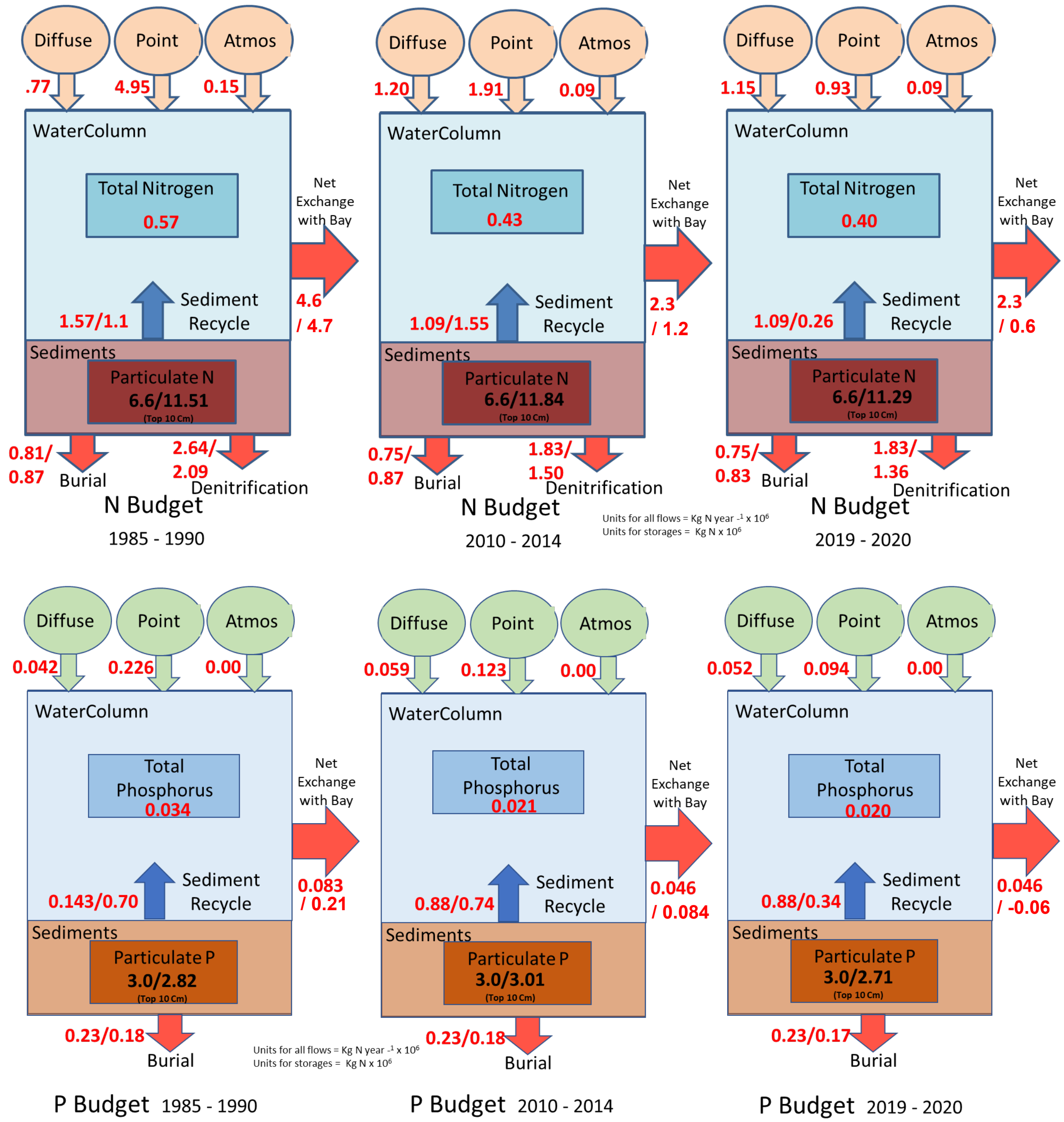

Figure 20: Nutrient budgets for nitrogen and phosphorus during three representative time periods in the Patapsco River estuary corresponding to a high-wastewater loading time period (1985-1990), reduced point source load period (2010-2014), and a period after upgrades to the Patapsco River WWTP (2019-2020). Note, the *Net Exchange With Bay* estimates include the Chesapeake Bay Water Quality and Sediment Transport Model computed exchanges (top number) and estimates from a one-layer box model (bottom number). *Please refer to Methods for data sources and methods.*